ISSN 2410-3438

Volume 9, Issue 24 – January – June – 2022

Journal of Quantitative and Statistical Analysis

ECORFAN®

Journal of Quantitative and Statistical Analysis, Volume 9, Issue 24, June 2022, is a journal edited six monthly by ECORFAN-Bolivia. 21 Loa 1179, Cd. Sucre. Chuquisaca, Bolivia. WEB: www.ecorfan.org, revista@ecorfan.org. Chief Editor: MIRANDA - TORRADO, Fernando. PhD. ISSN-On line: 2410-3438. Responsible for the latest update of this number ECORFAN Computer Unit. ESCAMILLA-BOUCHÁN, Imelda. PhD, LUNA-SOTO, Vladimir. PhD. Loa 1179, Cd. Sucre. Chuquisaca, Bolivia, last updated June 30, 2022.

The opinions expressed by the authors do not necessarily reflect the views of the editor of the publication.

Journal of Quantitative and Statistical Analysis

Definition of Journal

Scientific Objectives

Support the international scientific community in its written production Science, Technology and Innovation in the Field of Physical Sciences Mathematics and Earth sciences, in Subdisciplines of statistical analysis data analysis, multivariate analysis, statistic’s and probability, statistical analytical, calculation.

ECORFAN-Mexico SC is a Scientific and Technological Company in contribution to the Human Resource training focused on the continuity in the critical analysis of International Research and is attached to CONACYT-RENIECYT number 1702902, its commitment is to disseminate research and contributions of the International Scientific Community, academic institutions, agencies and entities of the public and private sectors and contribute to the linking of researchers who carry out scientific activities, technological developments and training of specialized human resources with governments, companies and social organizations.

Encourage the interlocution of the International Scientific Community with other Study Centers in Mexico and abroad and promote a wide incorporation of academics, specialists and researchers to the publication in Science Structures of Autonomous Universities - State Public Universities - Federal IES - Polytechnic Universities - Technological Universities - Federal Technological Institutes - Normal Schools - Decentralized Technological Institutes - Intercultural Universities - S & T Councils - CONACYT Research Centers.

Scope, Coverage and Audience

Journal of Quantitative and Statistical Analysis is a Journal edited by ECORFAN-Mexico S.C in its Holding with repository in Bolivia, is a scientific publication arbitrated and indexed with semester periods. It supports a wide range of contents that are evaluated by academic peers by the Double-Blind method, around subjects related to the theory and practice of statistical analysis data analysis, multivariate analysis, statistic’s and probability, statistical analytical, calculation with diverse approaches and perspectives, that contribute to the diffusion of the development of Science Technology and Innovation that allow the arguments related to the decision making and influence in the formulation of international policies in the Field of Physical Sciences Mathematics and Earth sciences. The editorial horizon of ECORFAN-Mexico® extends beyond the academy and integrates other segments of research and analysis outside the scope, as long as they meet the requirements of rigorous argumentative and scientific, as well as addressing issues of general and current interest of the International Scientific Society.

Arbitration Committee

Assignment of Rights

The sending of an Article to Journal of Quantitative and Statistical Analysis emanates the commitment of the author not to submit it simultaneously to the consideration of other series publications for it must complement the Originality Format for its Article.

The authors sign the Authorization Format for their Article to be disseminated by means that ECORFAN-Mexico, S.C. In its Holding Bolivia considers pertinent for disclosure and diffusion of its Article its Rights of Work.

Declaration of Authorship

Indicate the Name of Author and Coauthors at most in the participation of the Article and indicate in extensive the Institutional Affiliation indicating the Department.

Identify the Name of Author and Coauthors at most with the CVU Scholarship Number-PNPC or SNI-CONACYT- Indicating the Researcher Level and their Google Scholar Profile to verify their Citation Level and H index.

Identify the Name of Author and Coauthors at most in the Science and Technology Profiles widely accepted by the International Scientific Community ORC ID - Researcher ID Thomson - arXiv Author ID - PubMed Author ID - Open ID respectively.

Indicate the contact for correspondence to the Author (Mail and Telephone) and indicate the Researcher who contributes as the first Author of the Article.

Plagiarism Detection

All Articles will be tested by plagiarism software PLAGSCAN if a plagiarism level is detected Positive will not be sent to arbitration and will be rescinded of the reception of the Article notifying the Authors responsible, claiming that academic plagiarism is criminalized in the Penal Code.

Arbitration Process

All Articles will be evaluated by academic peers by the Double Blind method, the Arbitration Approval is a requirement for the Editorial Board to make a final decision that will be final in all cases. MARVID® is a derivative brand of ECORFAN® specialized in providing the expert evaluators all of them with Doctorate degree and distinction of International Researchers in the respective Councils of Science and Technology the counterpart of CONACYT for the chapters of America-Europe-Asia- Africa and Oceania. The identification of the authorship should only appear on a first removable page, in order to ensure that the Arbitration process is anonymous and covers the following stages: Identification of the Journal with its author occupation rate - Identification of Authors and Coauthors - Detection of plagiarism PLAGSCAN - Review of Formats of Authorization and Originality-Allocation to the Editorial Board-Allocation of the pair of Expert Arbitrators-Notification of Arbitration -Declaration of observations to the Author-Verification of Article Modified for Editing-Publication.

Istructions for Scientific, Technological and Innovation Publication

Knowledge Area

The works must be unpublished and refer to topics of statistical analysis data analysis, multivariate analysis, statistics and probability, statistical analytical, calculation and other topics related to Physical Sciences Mathematics and Earth sciences.

Presentation of the content

In the first article we present *Photoluminescence comparison of CNTs-SRO and GO-SRO films deposited on silicon substrates*, by MENDOZA-CONDE, Gabriel Omar, LUNA-LÓPEZ, José Alberto, HERNÁNDEZ-SIMÓN, Zaira Jocelyn and HERNÁNDEZ-DE LA LUZ, José Álvaro David, with adscription in the Benemérita Universidad Autónoma de Puebla, in the next article we present *Analysis of the behavior for polyethylene terephthalate (PET) in compression efforts for use in the masonry*, by VEGA-GUTIÉRREZ, Rebeca Eloísa, MARTÍNEZ-CARRILO, Irma, JUÁREZ-TOLEDO, Carlos and JIMÉNEZ-BETANCOURT, Ramón Octavio, with adscription in the Universidad Autónoma del Estado de México and Universidad Autónoma de Colima, in the next article we present *Thermodynamic analysis of a Stirling cycle with nuclear heat source for aerospace applications*, by DÍAZ-ESPINOZA, Gerardo, GALLARDO-VILLARREAL, José Manuel and VALLE-HERNÁNDEZ, Julio, with adscription in the Universidad Politécnica Metropolitana de Hidalgo and Universidad Autónoma del Estado de Hidalgo, in the next article we present *Brake systems tribological analysis and their evolution in sustainable characterization*, by LAGOS-LÓPEZ, Lorena, CRUZ-GOMEZ, Marco Antonio, MEJÍA-PÉREZ, José Alfredo and ESPINOSA-CARRASCO, María del Rosario, with adscription in the Benemérita Universidad Autónoma de Puebla.

Content

Article **Journal of Quantitative and Statistical Analysis**
June 2022, Vol.9 No.24 1-7

Photoluminescence comparison of CNTs-SRO and GO-SRO films deposited on silicon substrates

Comparación de la fotoluminiscencia de películas CNT-SRO y GO-SRO depositadas sobre sustratos de silicio

MENDOZA-CONDE, Gabriel Omar†, LUNA-LÓPEZ, José Alberto*, HERNÁNDEZ-SIMÓN, Zaira Jocelyn and HERNÁNDEZ-DE LA LUZ, José Álvaro David

Benemérita Universidad Autónoma de Puebla, Centro de Investigaciones en Dispositivos Semiconductores (CIDS-ICUAP), Av. San Claudio y 14 sur, Edificios IC5 y IC6, C. U., Col. San Manuel, Puebla, Pue. 72570, México.

ID 1st Author: *Gabriel Omar, Mendoza-Conde* / **ORC ID:** 0000-0001-5451-9770, **CVU CONACYT ID:** 774931

ID 1st Co-author: *José Alberto, Luna-López* / **ORC ID:** 0000-0002-7647-3184, **CVU CONACYT ID:** 200808

ID 2nd Co-author: *Zaira Jocelyn, Hernández-Simón* / **ORC ID:** 0000-0003-4185-4101, **CVU CONACYT ID:** 774431

ID 3rd Co-author: *José Álvaro David, Hernández-De la Luz* / **ORC ID:** 0000-0002-7913-0240, **CVU CONACYT ID:** 240901

DOI: 10.35429/JQSA.2022.24.9.1.7 Received January 10, 2022; Accepted June 30, 2022

Abstract

In this work, we make a comparative study of the photoluminescence (PL) obtained from the structures formed by carbon nanotubes (CNTs) and graphene oxide (GO) deposited by Spin Coating on silicon rich oxide (SRO) thin films which were obtained by hot filament chemical vapor deposition (HFCVD) technique. The objective of building these hybrid structures is to increase the photoluminescence response. The PL measurements show that the CNTs-SRO heterostructures exhibit a stronger photoluminescence when compared to that obtained from the GO-SRO heterostructure, similar behaviour exhibit the GO-CNTs/SRO ones when compared to the CNTs-GO/SRO ones. It is worthy to note that the CNTS-SRO structures PL displays blue light emission, while green light emission is present in the CNT-GO ones. By deconvolution of the PL spectra, we identify the emission mechanisms present in graphene oxide, carbon nanotubes layers and the silicon rich oxide films. Due to the good properties of PL exhibited by the CNTs-SRO and GO-CNTs/SRO structures, they are excellent candidates to be applied in the field of photonic and electroluminescent devices.

SRO, HFCVD, Photoluminescence

Resumen

En este trabajo, se realizó un estudio comparativo de la fotoluminiscencia (FL) de nanotubos de carbono (CNTS) y óxido de grafeno (GO) depositados por Spin Coating y películas de óxido de silicio rico en silicio (SRO) depositadas mediante la técnica de depósito químico en fase vapor asistido por filamento caliente (HFCVD). Para mejorar la respuesta de la fotoluminiscencia, se combinaron los CNTs y el GO para formar un hibrido de estos dos materiales. Los espectros muestran que la heteroestructura CNTs-SRO muestra una fotoluminiscencia más alta en comparación con la GO-SRO, mientras que la estructura GO-CNTS/SRO muestra una respuesta fotoluminiscente más alta que la estructura CNTs-GO/SRO. Los espectros muestran que los CNTs emiten luz azul, mientras que la luz verde domina en el híbrido CNTs-GO. A través de la deconvolución de los espectros de PL, se obtuvieron los mecanismos de emisión presentes en las capas de GO, CNTS y la película de SRO. Por lo tanto, debido a estos resultados, las heteroestructuras con CNTs (CNTs-SRO and GO-CNTs/SRO) presentan un gran potencial de aplicación en el campo de los dispositivos fotónicos y electroluminiscentes.

SRO, HFCVD, Fotoluminiscenc

Citation: MENDOZA-CONDE, Gabriel Omar, LUNA-LÓPEZ, José Alberto, HERNÁNDEZ-SIMÓN, Zaira Jocelyn and HERNÁNDEZ-DE LA LUZ, José Álvaro David. Photoluminescence comparison of CNTs-SRO and GO-SRO films deposited on silicon substrates. Journal of Quantitative and Statistical Analysis. 2022. 9-24:1-7.

* Correspondence to the Author (E-mail: jose.luna@correo.buap.mx)
† Researcher contributing as first Author.

June 2022, Vol.9 No.24 1-7

Introduction

One of the most technologically interesting materials is silicon-rich oxide (SRO), which is considered to be a material with great potential for the fabrication of optoelectronic devices because it is a material compatible with CMOS technology. In addition to various methods can be used to obtain the SRO, such as LPCVD, PEVCD, HFCVD, implantation of silicon in SiO_2, sputtering, etc. [1].

A relevant characteristic of the SRO is that it facilitates the formation of silicon nanocrystals embedded in a SiO_2 matrix [2], which generate low dimensional effects and therefore, an efficient emission of light [1]. The SRO possesses interesting structural, optical, and electrical properties which can be tailored by the silicon excess and defects contained in the films [3]. The incorporation of silicon into SiO_x modifies its bandgap as well as its optical properties such as photoluminescence, absorption and emission of light. The latter is attributed to quantum effects present in silicon nanocrystals and localized defects at the interface between nanocrystals and silicon matrix [4].

On the other hand, carbon nanostructures such as fullerenes, carbon nanotubes (CNTs), nanodiamond (ND) films, and graphene oxide (GO) are very attractive functional groups in the fabrication of important optoelectronic devices such as sensors, field emitters, and light-emitting applications [5]. Luminescent carbon nanostructures are also expected to achieve high-efficiency photoluminescence in light-emitting devices and low toxicity in biological and biomedical applications [6].

There are two types of CNTs; single-wall carbon nanotubes (SWCNTs) and multi-wall carbon nanotubes (MWCNTs). MWCNT is a CNT structure consisting of several coaxially concentric shells of graphene sheets rolled up. In both cases, their one-dimensional structure, interlayer interaction and curvature effects lead to many extraordinary mechanical, electrical, optical, thermal and chemical properties. All of this makes them suitable for enhancing the functionalization of existing materials and even creating other heterostructures. Furthermore, CNTs thin films are electrically conductive and transparent, and have recently been used as ohmic contacts in GaN and organic materials [7].

In this context, the SRO may be used to realize novel heterostructures using CNTs to improve its optical properties. On the other hand, Graphene oxide is a bidimensional carbon-based material that can be used in graphene-based optoelectronic devices, especially for biomedical applications, due to its unique electronic properties and large specific surface area [8, 9]. Since graphene has no band gap as an intrinsic material, it is not expected to exhibit photoluminescence due to relaxation of excited carriers; however, when, it is functionalized, such as graphene oxide, it has a band gap and exhibits photoluminescence [10]. Therefore, the GO may be used to form new structures in order to enrich their optical properties.

Thus, by using CNTs and GO along with the SRO it is possible to make up nanostructured materials which may be of great interest because of their outstanding photoluminescent properties based on the quantum effects due to low dimensions and energy band structures. Thus, these photoluminescent properties may be focused on forming new light-emitting devices in the field of optoelectronics.

Development and methodology

CNTs and GO thin films were deposited on n-type crystalline silicon substrates with 100 orientation and <0.005 Ω-cm resistivity by the spin-coating method shown in Figure 1. The substrate is subjected to a MOS cleaning process (RCA standard) [11]. Si/CNTs, Si/GO, Si/CNTs-GO and Si/GO-CNTs structures were obtained. All structures to be deposited (CNTs and GO) are dissolved in an alcoholic solvent, in this case methanol, due to the low molarity, to avoid aggregation of the particles to be deposited, in the case of GO and CNTs, according to the report [12], because ideal solvents for dispersing graphene are those that minimize the interfacial tension between graphene and the solvent.

For the deposition of each layer of solvent and solute, it was attached to a Si substrate on a rotating plate, and then solution droplets were deposited on the substrate and rotated at a certain speed with a motor mounted on the plate. A certain angular velocity in order to create a thin film of solution by centrifugal force.

ISSN: 2410-3438

The parameters used for thin film deposition are as follows: the first speed is 700 rpm for a deposition time of 10 s, and the second speed is 3000 rpm for 15 s to deposit 3 drops of the solution, using methanol as the solvent and repeat the process three times. The concentrations of CNTs and GO solutions were 1.8 g/L and 1.3 g/L, respectively.

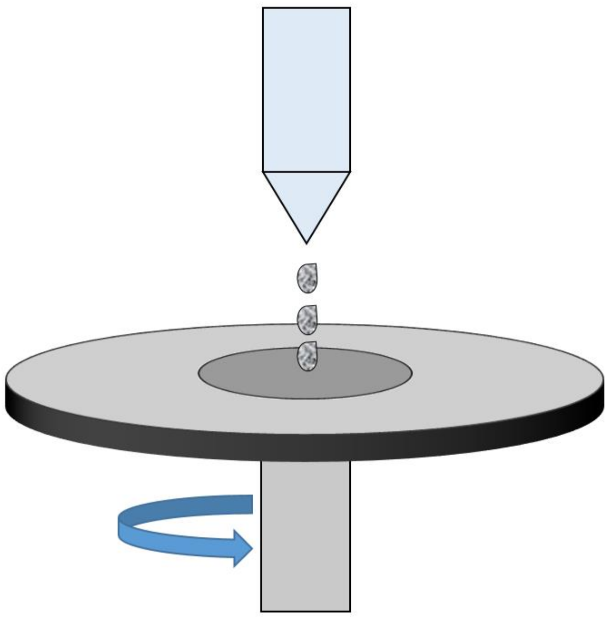

Figure 1 Spin coating process

The SRO films were deposited on the Si/CNTs, Si/GO, Si/CNTs-GO and Si/GO-CNTs structures using a HFCVD (Hot Filament Chemical Vapor Deposition) reactor. These depositions were carried out with a constant flow of molecular hydrogen (H_2) at 100 sccm level, the source-to-substrate distance (ssd) was kept at 7 mm. Some parameters were fixed during the deposition process, such as the filament-to-source distance (fsd), which was kept constant at 8 mm, the deposition time (td) was 1 min, the voltage applied to the filaments was 84 V and the system pressure at one atmosphere.

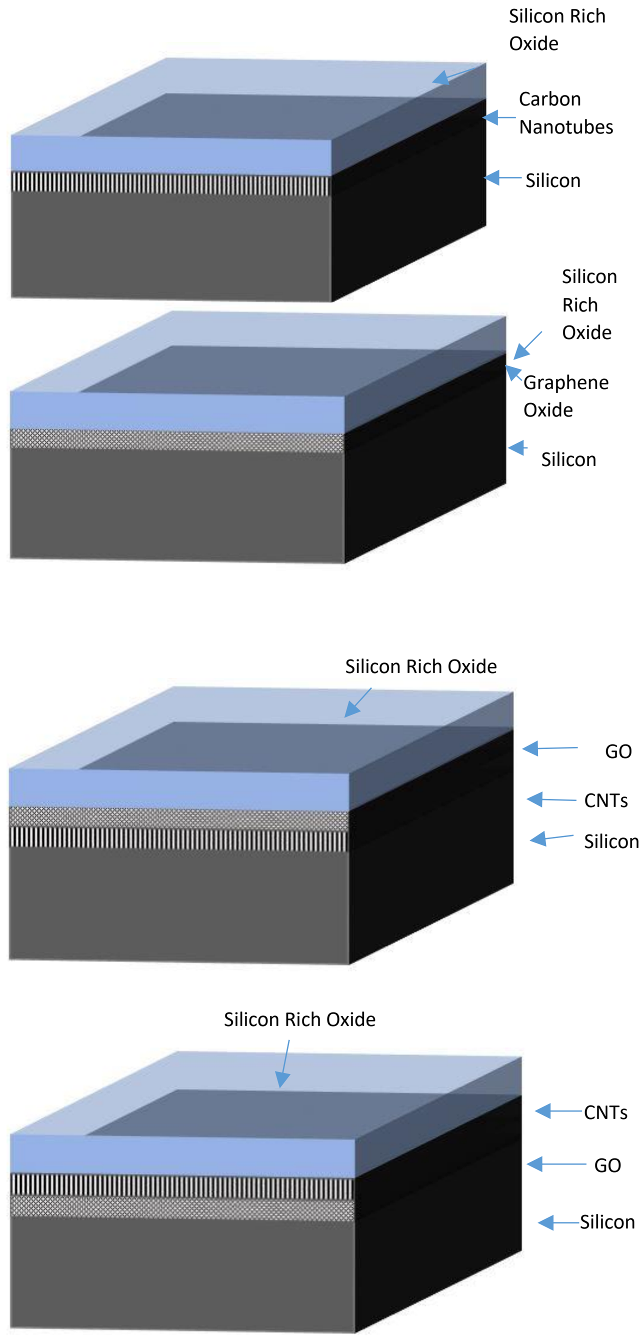

Figure 2 Scheme of the 4 manufactured structures

Using photoluminescence (PL) spectroscopy, emission spectra were obtained and emission-related defects were identified. Spectra were acquired on a Horiba Jobin Yvon FluroMax 3 fluorescence spectrophotometer equipped with a 150 W xenon excitation lamp, 0.3 nm resolution, 370-1000 nm range, and high sensitivity emission detector. Measurements were performed under excitation at 330 nm.

June 2022, Vol.9 No.24 1-7

Results and analysis

Graph 1 shows the photoluminescence spectrum of the Si/CNTs/SRO structure, and the inset shows the photoluminescence spectrum of the Si/GO/SRO structure. The PL intensity of the Si/CNTs/SRO structure shows a strong and well-defined peak in blue (450 nm), which is attributed to the CNTs, in addition, a lower intensity peak can be seen in the red band around 750 nm. For Si/GO/SRO structure two peaks appeared, a more defined peak around 420 nm was attributed to GO, just like in the structure with CNT, a smaller peak appeared around 750 nm, and this is a characteristic of SRO films.

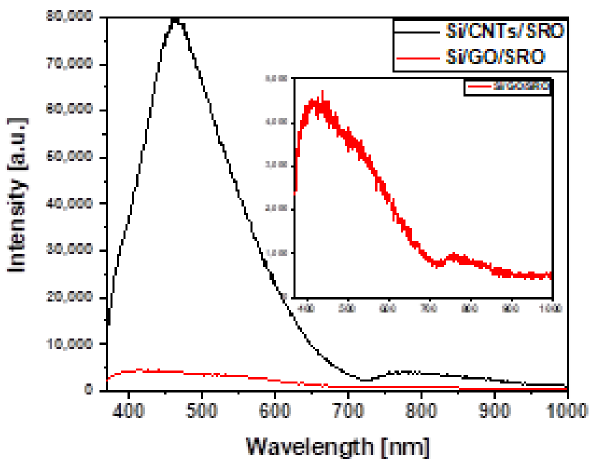

Graphic 1 PL spectra of the Si/CNTs/SRO and Si/GO/SRO structures

Graphic 2 shows the photoluminescence spectrum of the Si/GO-CNTs/SRO structure, and the inset shows the photoluminescence spectrum of the Si/CNTs-GO/SRO structure. The PL intensity of the Si/GO-CNTs/SRO structure shows a strong and clear green peak (519 nm), which is attributed to the existence of the GO-CNTs composite [13]. For the Si/CNTs-GO/SRO structure, two peaks are shown, a more defined peak around 400 nm is attributed to GO, and another weaker peak around 750 nm and as mentioned above, is characteristic of SRO films. As can be seen from the inset figure, the photoluminescence emission decreases when the carbon nanotubes layer is covered with graphene oxide particles. The latter produces a quenching effect.

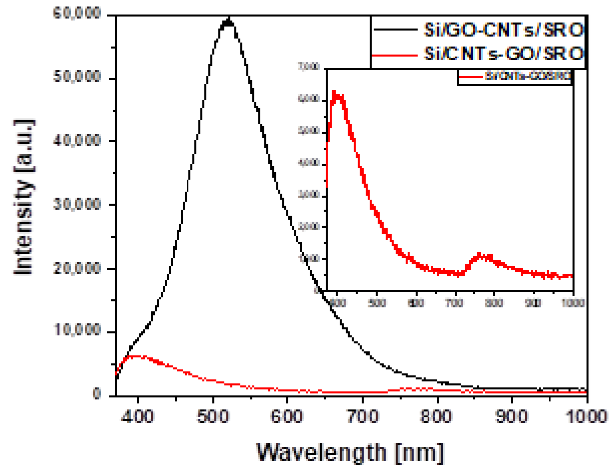

Graphic 2 PL spectra of the Si/GO-CNTs/SRO and Si/CNTs-GO/SRO structures.

As shown in Graphics 1 and 2, the photoluminescence spectrum is very broad, suggesting that multiple emission mechanisms may be involved. To find all possible contributions to the photoluminescence process in the structure, the deconvolution of each spectrum is shown in Graph 3. The different peaks defined by the deconvolution are associated with different types of defects, as shown below, with their respective positions in energy, see Table 1.

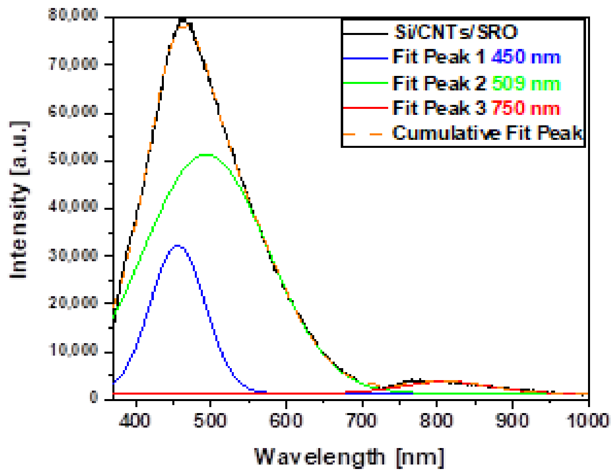

Graphic 3 Deconvoluted spectra of the Si/CNTs/SRO structure

CNTs/SRO photoluminescence emission mechanisms.	
Luminescent centers associated with diamond films	450 nm [13]
Defects due to Nitrogen	509 nm [14]
Nonbridging oxygen hole centers	750 nm [15]
GO/SRO photoluminescence emission mechanisms.	
It is attributed to the excimer present in the GO	405 nm [16]
Interactions between graphene planes and OD (Oxidative debris)	495 nm [16]
Nonbridging oxygen hole centers	750 nm [15]

Table 1 Types of defects linked to the position of the PL peaks of the structures

Table 1 shows the emission mechanisms associated with CNTS, GO and SRO, two mechanisms have been identified for carbon nanotubes, one in the blue region at 450 nm and the other in the green region, likewise, graphene oxide exhibits two emission mechanisms, the first in the purple region (405 nm) and the other in the green region (495 nm). Finally, a peak associated to nonbridging oxygen hole centers (NBOHC) was identified for silicon rich oxide. In the structures with CNTs and GO, both a photoluminescence shift and a stronger emission is observed for the case of CNTs contribution because in these structures both curvature effects and inter-walls interaction as well as the edge effects and chiral indexes (n,m) modify significantly their electronic structure which favors the electronic transitions and therefore the radiative emission [17]. Blue-green photoluminescence has been previously observed in diamond films [14]. The blue luminescence is thought to be due to nitrogen contamination, as N-bonded carbons have been reported to act as luminescent centers in CNTs, similar to N-defects in CVD-derived nanodiamonds, as well as in natural diamond [14]. In general, CVD-derived carbon nanotubes and diamond are known to contain nitrogen and nitrogen-related defects [14], so the spectra suggest that the photoluminescence of the samples may have a similar origin based on nitrogen-bonded carbon, although the predominant phase in the samples is sp2-bonded carbon [14]. The C=O functional groups present on the surface of carbon nanotubes are responsible for the green emission. [13].

Graphene oxide exhibits two emission bands at 405 nm and 495 nm, respectively. These bands are similar to those reported in literature. [16]. Graphene oxide contains highly oxidized polycyclic aromatic hydrocarbon fragments, called oxidative debris (OD), which are present in graphene oxide, and they are attached to graphene oxide in a graphene-like plane [16]. OD has oxygen-containing groups like GO, so oxygen-containing groups should not be a direct source of the 495 nm band. Therefore, it is reasonable to attribute the 495 nm band to the interaction between the graphic plane and OD. The emission mechanism at 405 nm is due to the formation of excimer molecules, which can occur between polyaromatic molecules and conjugated polymers. Similarly, excimers can form GO sheets through π−π overlap [16].

Oxygen-containing groups in GO, such as carboxyl or epoxy groups, always induce non radiative electron-hole pair recombination, making the emission intensity of GO very weak. [17]. The deposited SRO films show weak emission. However, the observed photoluminescence emission has a peak around 750 nm, which proves that the PL emission does not occur via interband recombination.

Therefore, emission through localized states present in nonbridging oxygen hole centers is the most likely mechanism [15]. As shown in Figure 4, when CNT was combined with GO, as described above, a shift of photoluminescence emission towards 500 nm was observed in the structure of CNTs in the upper part, which was due to the functional group C=O, except that the addition of GO did not increase the emission. On the other hand, in the structure with CNT and GO on top, the emission is similar to that of graphene oxide and is not affected by the interaction with carbon nanotubes. While for both heterostructures, the 750 nm peak associated with the SRO thin film still exists.

Conclusions

The photoluminescence properties of CNTs, GO, and SRO thin film layers and heterostructures formed from these materials were investigated and compared. The photoluminescence spectra show the emission of CNTs in the blue-green region, which is thought to be caused by contamination caused by nitrogen binding to carbon in the blue region, and the characteristic green-emitting functional groups of CNTs due to C=O. GO emission was observed in two bands, 405 and 495 nm, caused by oxidative debris and excimers, respectively. Whereas for the SRO film, a contribution of 750 nm due to nonbridging oxygen hole centers is present. In the structure of mixed CNT and GO, the emission shift and its shielding are observed, which is due to the presence of nitrogen defects in the CNTs, whereas for the structure with GO on top, the emission is the same as that of GO without carbon nanotubes. Structures with CNTs have great potential in light-emitting device applications due to their good emission behavior.

Acknowledgements

The authors acknowledge CIDS and INAOE laboratories for their help in the samples characterizations.

Funding

This work has been financed by CONACYT [grant number: 731871]

References

[1] Martínez, H., Luna, J., Morales, R., Casco, J., Hernández, J., & Luna, A. et al. (2021). Blue Electroluminescence in SRO-HFCVD Films. *Nanomaterials, 11*(4), 943. https://doi.org/10.3390/nano11040943

[2] Simón, Z., López, J., de la Luz, Á., Salgado, G., Leyva, K., & López, J. et al. (2021). SiOx films deposited by HFCVD: Their conduction response to light and intrinsic photovoltaic effect. *Surfaces And Interfaces, 26*, 101411. https://doi.org/10.1016/j.surfin.2021.101411

[3] Hernández Simón, Z., Luna López, J., de la Luz, A., Pérez García, S., Benítez Lara, A., & García Salgado, G. et al. (2020). Spectroscopic Properties of Si-nc in SiOx Films Using HFCVD. *Nanomaterials, 10*(7), 1415. https://doi.org/10.3390/nano10071415

[4] Martínez Hernández, H., Luna López, J., Hernández de la Luz, J., Luna Flores, A., Monfil Leyva, K., & García Salgado, G. et al. (2020). Spectroscopic and Microscopic Correlation of SRO-HFCVD Films on Quartz and Silicon. *Crystals, 10*(2), 127. https://doi.org/10.3390/cryst10020127

[5] Avouris, P., Freitag, M., & Perebeinos, V. (2008). Carbon-nanotube photonics and optoelectronics. *Nature Photonics, 2*(6), 341-350. https://doi.org/10.1038/nphoton.2008.94

[6] Cayuela, A., Soriano, M., & Valcárcel, M. (2015). Photoluminescent carbon dot sensor for carboxylated multiwalled carbon nanotube detection in river water. *Sensors And Actuators B: Chemical*, 207, 596-601. https://doi.org/10.1016/j.snb.2014.10.102.

[7] Lee, K., Wu, Z., Chen, Z., Ren, F., Pearton, S., & Rinzler, A. (2004). Single Wall Carbon Nanotubes for p-Type Ohmic Contacts to GaN Light-Emitting Diodes. *Nano Letters, 4*(5), 911-914.https://doi.org/10.1021/nl0496522

[8] Montes-Navajas, P., Asenjo, N., Santamaría, R., Menéndez, R., Corma, A., & García, H. (2013). Surface Area Measurement of Graphene Oxide in Aqueous Solutions. *Langmuir, 29*(44), 13443-13448. https://doi.org/10.1021/la4029904

[9] Han, J., Kim, J., Jo, S., Kim, S., Kim, J., & Kang, B. et al. (2012). Graphene oxide as a multi-functional p-dopant of transparent single-walled carbon nanotube films for optoelectronic devices. *Nanoscale, 4*(24), 7735. https://doi.org/10.1039/c2nr31923c

[10] Jin, Y., Zheng, Y., Podkolzin, S., & Lee, W. (2020). Band gap of reduced graphene oxide tuned by controlling functional groups. *Journal Of Materials Chemistry C, 8*(14), 4885-4894. https://doi.org/10.1039/c9tc07063j

[11] Ruzyllo, J. (2004). *Cleaning technology in semiconductor device manufacturing VIII*. Pennington, New Jersey: Electrochemical Society.

[12] Wang, W., Ruderer, M., Metwalli, E., Guo, S., Herzig, E., Perlich, J., & Müller-Buschbaum, P. (2015). Effect of Methanol Addition on the Resistivity and Morphology of PEDOT:PSS Layers on Top of Carbon Nanotubes for Use as Flexible Electrodes. ACS *Applied Materials &Amp; Interfaces, 7*(16), 8789-8797. https://doi.org/10.1021/acsami.5b01327

[13] Fedoseeva, Y., Bulusheva, L., Okotrub, A., Kanygin, M., Gorodetskiy, D., & Asanov, I. et al. (2015). Field emission luminescence of nanodiamonds deposited on the aligned carbon nanotube array. *Scientific Reports, 5*(1). https://doi.org/10.1038/srep09379

[14] Zhou, J., Zhou, X., Li, R., Sun, X., Ding, Z., Cutler, J., & Sham, T. (2009). Electronic structure and luminescence center of blue luminescent carbon nanocrystals. *Chemical Physics Letters, 474*(4-6), 320-324. https://doi.org/10.1016/j.cplett.2009.04.075

[15] Vaccaro, L., Cannas, M., & Radzig, V. (2009). Luminescence properties of nonbridging oxygen hole centers at the silica surface. *Journal Of Non-Crystalline Solids*, *355*(18-21), 1020-1023. https://doi.org/10.1016/j.jnoncrysol.2008.11.028

[16] Du, D., Song, H., Nie, Y., Sun, X., Chen, L., & Ouyang, J. (2015). Photoluminescence of Graphene Oxide in Visible Range Arising from Excimer Formation. *The Journal Of Physical Chemistry C, 119*(34), 20085-20090. https://doi.org/10.1021/acs.jpcc.5b04529

[17] Liu, F., Cao, Y., Yi, M., Xie, L., Huang, W., & Tang, N. et al. (2013). Thermostability, Photoluminescence, and Electrical Properties of Reduced Graphene Oxide–Carbon Nanotube Hybrid Materials. *Crystals, 3*(1), 28-37. https://doi.org/10.3390/cryst3010028.

Article
Journal of Quantitative and Statistical Analysis
June 2022, Vol.9 No.24 8-14

Analysis of the behavior for polyethylene terephthalate (PET) in compression efforts for use in the masonry

Análisis del comportamiento del tereftalato de polietileno (PET) en esfuerzos de compresión para su uso en la mampostería

VEGA-GUTIÉRREZ, Rebeca Eloísa†*, MARTÍNEZ-CARRILO, Irma, JUÁREZ-TOLEDO, Carlos and JIMÉNEZ-BETANCOURT, Ramón Octavio

Universidad Autónoma del Estado de México, Professional Academic Unit Tianguistenco, Mexico.
Universidad Autónoma de Colima, Faculty of Mechanical and Electrical Engineering, Mexico.

ID 1st Author: *Rebeca Eloísa, Vega-Gutiérrez* / **ORC ID**: 0000-0003-3274-0743

ID 1st Co-author: *Irma, Martínez-Carrillo* / **ORC ID**: 0000-0002-7952-4418, **Researcher ID Thomson**: B-9264-2016, **CVU CONACYT ID**: 39914

ID 2nd Co-author: *Carlos, Juárez-Toledo* / **ORC ID**: 0000-0002-7440-3246, **Researcher ID Thomson**: C-1368-2016, **CVU CONACYT ID**: 39912

ID 3rd Co-author: *Ramón Octavio, Jiménez-Betancourt* / **ORC ID**: 0000-0002-0171-7279, **CVU CONACYT ID**: 88193

DOI: 10.35429/JQSA.2022.24.9.8.14 Received January 15, 2022; Accepted June 30, 2022

Abstract

This article focuses on analysis and a study on the mechanical behavior of recycled plastic materials to manufacture bricks. The current proposal provides a viable alternative for the manufacture of bricks under its regulations, standards and care for the environment. Standardized tests for the study and analysis of the behavior of polyethylene terephthalate (PET) in compressive stresses also is showing. SolidWorks finite element analysis is used to validate the regulations of the bricks, where the results obtained show the values within the norm. The implementation of models is presented through simulations of the proposed brick based on these materials within the masonry. Finally, a methodology for the treatment of PET and its transformation process for the manufacture of partitions with polyethylene terephthalate is proposed. In addition, a methodology for the treatment of PET and its transformation process for the manufacture of partitions with polyethylene terephthalate is proposed.

Polyethylene terephthalate (PET), Compressive stresses and masonry

Resumen

En este artículo se realiza un estudio y análisis sobre el comportamiento mecánico de los materiales plásticos reciclados para ser considerados como posible materia prima para fabricar ladrillos. La propuesta actual proporciona una alternativa viable para la fabricación de ladrillos bajo sus normatividades, estándares y al cuidado del medio ambiente. También se enumeran las pruebas estandarizadas para el estudio y análisis del comportamiento del tereftalato de polietileno (PET) en esfuerzos de compresión, así como su aplicación por medio del elemento finito con ayuda del software SolidWorks, para validar si los resultados obtenidos de las variables evaluadas muestran el valor mínimo que debe de cumplir la norma. Se presenta la implementación de modelos por medio de simulaciones del ladrillo propuesto en base de dichos materiales dentro de la mampostería. Finalmente, se propone una metodología para el tratamiento del PET y su proceso de transformación para la manufactura de tabiques con tereftalato de polietileno.

Tereftalato de polietileno (PET), Esfuerzos de compresión y mampostería

Citation: VEGA-GUTIÉRREZ, Rebeca Eloísa, MARTÍNEZ-CARRILO, Irma, JUÁREZ-TOLEDO, Carlos and JIMÉNEZ-BETANCOURT, Ramón Octavio. Analysis of the behavior for polyethylene terephthalate (PET) in compression efforts for use in the masonry. Journal of Quantitative and Statistical Analysis. 2022. 9-24:8-14.

* Correspondence to the Author (E-mail: rvegag439@alumno.uaemex.mx)
† Researcher contributing as first Author.

Article **Journal of Quantitative and Statistical Analysis**
June 2022, Vol.9 No.24 8-14

Introduction

The issue of pollution by plastics has increased due to the lack of awareness and responsibility towards the environment when they are discarded, which are made of materials that are resistant to degradation, in any geographical space; avoiding the application of reprocessing to give them another favourable use.

Consequently, this waste invades natural landscapes, causing harmful impacts on the living beings that inhabit them, such as the release of substances that nature cannot assimilate. The combustion of this waste generates toxic gases, and thus more pollution [1].

The search for alternatives to contribute to the care of the environment has been an issue highlighted in social and industrial spheres to implement an environmental culture, making solid urban waste, especially plastics, become new sustainable materials that serve as raw materials to manufacture more environmentally friendly products for the field of housing construction due to the high population growth. In view of this, it is evident to promote technology towards the design of solid and infrastructural objects such as building bricks where the main recyclable plastic waste is required as raw material, considering the analysis of their selection by means of the mechanical properties they possess.

Masonry

The term masonry refers to a construction of bricks placed in mortar to be laid in rows or courses, and if these are laid on top of each other they form a brick wall [2].

Within construction, brick is the most commonly used element as it is a masonry of small dimensions to be placed manually to build larger elements such as walls [3].

One of the most important materials for ceramic bricks is clay due to the following characteristics [4]:

- Ease of use in simple and structural constructions.

- Good compressive strength.

- Multiple shapes with different levels of quality.

A. Characteristics of bricks

In the following, the quality requirements for bricks and ceramic blocks to be considered as masonry elements will be mentioned:

Manufacturing	With machine
Subtypes	Solid (compact throughout).
Quality grades	A
Structural requirements	Suitable for load-bearing masonry under advanced stresses.
Functional requirements	Suitable for exterior or interior use in single or double-sided apparent walls.
Minimum simple compressive strength (MPa)	20
Nominal dimensions of ceramic bricks and blocks in cm (length, width and height/profile)	20 X 20 *5
Dimensions of machine-made ceramic bricks and blocks in cm (length, width and height/perpallet)	19 X 19 X 4.5

Table 1 Requirements and characteristics of bricks according to N-CMT-2-01-001/02
Source: [5]

The mechanical properties of 20*20*5 cm clay brick are as follows [6]:

Properties	Clay brick
Dimensions (cm)	20 X 20 X 5
Water absorption (%)	23
Bulk density (kg/m3)	1,330
Modulus of elasticity (MPa)	5,300
Poisson's Coefficient	0.17
Shear modulus of elasticity (MPa)	-
Compressive strength (MPa)	5.3
Tensile strength (MPa)	0.53
Loading force (MPa)	-
Coefficient of thermal expansion (m/m/°C)	0.6×10^{-5}
Coefficient of friction of mortar joints (m/m/°C)	-
Tensile bond strength of mortar joints (MPa)	-
Adhesive shear strength (cohesion) of mortar joints (MPa)	-

Table 2 Mechanical properties of clay brick

ISSN: 2410-3438

Article
Journal of Quantitative and Statistical Analysis
June 2022, Vol.9 No.24 8-14

The compression test of the bricks should be in the range of 2000 to 5000 psi (15 to 35 MPa), if it is below this range the brick is of poor quality [7].

B. Environmental impact

Brick production benefits the profitability of the ceramic and construction industry, as well as satisfying the need for housing for the population; to some extent it reflects an environmental problem from the high energy consumption for its production to the emissions of toxic gases from its chimneys, causing an increase in the rate of pollution and detrimental damage to the health of workers. Given this, waste plastics can be proposed as a new solution to brick formation with the following advantages [8]:

- Not requiring the use of large-scale materials or facilities.
- Avoiding the felling of trees for firewood to run the kilns.
- Minimising air pollution.
- Increased production of green housing.

Evolution of polymers in the context of recycling

Classifications of recycled polymers are based on the thermal property that characterises their behaviour and processability; for example, thermoplastics have linear or branched structures where they facilitate conversion into fluids if heated to certain temperatures, representing high malleability into the desired shape upon cooling. Thermoplastics are considered to be the most widely applied and commercially used category of synthetic polymers; among them are: polyethylenes, polypropylenes, polyvinyl chloride, polycarbonates, polyurethanes, among others [9].

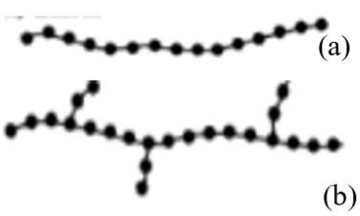

Figure 1 Molecular structure of thermoplastic polymers (a) linear such as acrylics, nylons, polyethylene and polyvinyl chloride (b) branched such as polyethylene
Source: [10]

The first step in recycling plastic waste from the urban environment is the "collection" of plastic waste through the various containers to landfill sites for sorting and cleaning. One of the best ways of collecting and separating plastics in recycling centres is to visualise the numerical code that the product has, as this allows the type of polymer the container is made of to be identified; they are even guided by the colour of the plastic [11]:

1	**PET**	Polyethylene terephthalate: Soft drink bottles and microwaveable ready meals trays.
2	**PHPE**	High density polyethylene: Milk bottles and dishwashing liquid.
3	**PVC**	Polyvinyl chloride: Food trays, plastic film and water bottles.
4	**LDPE**	Low density polyethylene: Plastic bags.
5	**PP**	Polypropylene: margarine containers.
6	**PS**	Polystyrene: Yoghurt containers, food trays, fast food containers, household appliance packaging.
7	**Others**	All other plastics: Melanin, used in household appliances.

Table 3 Code number to identify plastics
Source: [12]

Standardisation of recyclable plastics

In order to determine the minimum requirements for new materials made of polymers, they will have to undergo and comply with several standardised tests, among them the American Society for Testing and Materials (ASTM).

ASTM D695 determines the compressive strength of polymer-based materials. Within this standard, the dimensions 4 x 4 x 8 (cm) will be considered for PET thermoplastic [13].

One of the implementation models for the production of environmentally friendly bricks using recyclable plastics is based on the following flow chart [14]:

ISSN: 2410-3438

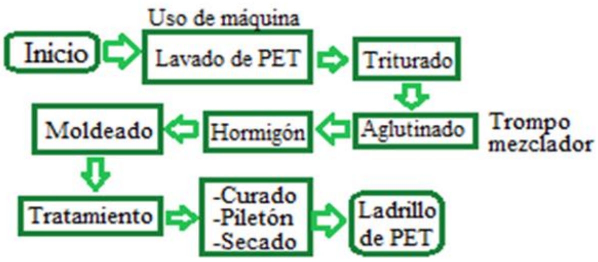

Figure 2 Process flow diagram for the production of environmentally friendly PET bricks

Methodology

The finite element method (FEM) is a numerical method that solves a system of partial derivative equations for the approximate resolution of continuous problems where the boundary equations, initial conditions, are established based on the discretisation of the problem domain in subdomains (elements), these are interconnected by a series of points (nodes). Therefore, it is translated as a system with different degrees of freedom whose behaviour is modelled from a system of linear equations; among them are:

- Stiffness matrix: it establishes the deformation relationship that defines the behaviour of an element subjected to a stress analysis. Its development is considered in terms of energy by the function:

$$U_e = \frac{1}{2}\int \sigma^T \epsilon A dx \quad (1)$$

- Stresses and deformation: When a body is deformed, the action of external force causing deformation at each point of the body generates a displacement; if this body is three-dimensional it is governed by the expression:

$$s = \mathrm{u}i + \mathrm{v}j + \mathrm{w}k \quad (2)$$

Where u, v, w; are displacements in the x, y, z directions.

The type of AutoFEM module to be used will be static analysis to perform stress state modelling for mechanical structures and strength testing [15].

Results

For the validation of the proposed process for the production of PET bricks, two simulations using SolidWorks finite element will be carried out for the following two cases:

1. Clay brick.

2. PET brick.

In both cases, their behaviour in compression will be analysed under the following considerations:

1. The standardised dimensions of PET and its mechanical properties are standardised from the SolidWorks database.

2. For the clay brick, the data in Table 2 will be used to determine the load forces (minimum and maximum) in relation to the area of the clay brick; these forces will be used for the PET brick according to its standardised dimensions by:

$$\sigma = \frac{F}{A} \text{ en } \left[\frac{N}{mm^2}\right] \quad (3)$$

Minimum Compression Limit (MPa)	15
Maximum Compressive Limit (MPa)	35
Nominal dimensions of the clay brick in mm (length, width and height or camber)	200x200x50
Area (mm^2)	40000
Minimum compressive strength (N)	6E+05
Maximum compressive strength (N)	1.40E+06

Table 4 Parameters of the clay brick to be used
Source: [16]

Figures 3 and 4 show the successive form tension behaviour of the clay brick and the PET brick.

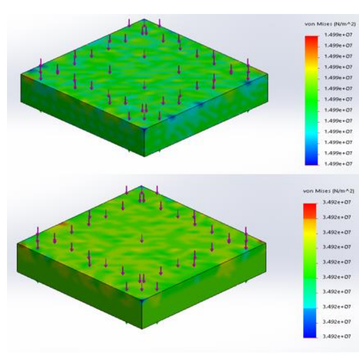

(a)

(b)

Figure 3 Tensile stress (Pa) (a) minimum (b) maximum for the clay brick
Source: Own elaboration

ISSN: 2410-3438

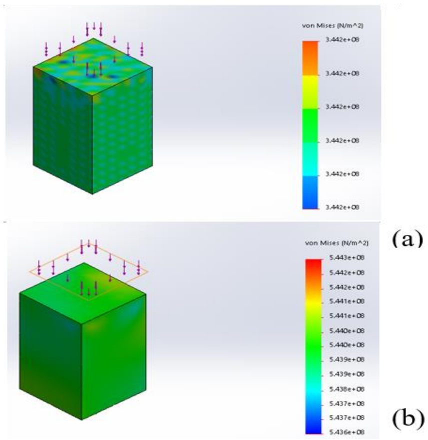

Figure 4 Tensile stress (Pa) (a) minimum (b) maximum for the PET brick
Source: Own elaboration

Figures 5 and 6 show successively the minimum and maximum displacement behaviour of the clay brick and the PET brick.

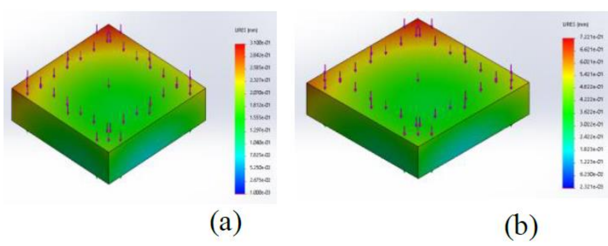

Figure 5 Displacement (mm) (a) minimum (b) maximum for the clay brick
Source: Own elaboration

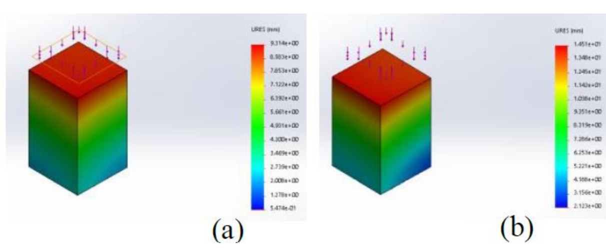

Figure 6 Displacement (mm) (a) minimum (b) maximum for the PET brick
Source: Own elaboration

Based on the results obtained for the tensile stress, it is shown that under a minimum compressive strength of 6E+05 N, the clay brick has a lower value than the PET brick (1.499e+07<3.442e+08Pa).

In the case of a maximum compressive strength of 1.40E+06 N, the clay brick has a lower value than the PET brick (3.492e+07<5.443e+08 Pa).

Within the displacement analysis, the same compressive strength limits of 6E+05N and 1.40E+06 N were used, of which reflected that the minimum displacement of clay is less than that of PET (3.100e-01<9.314e+00 mm) while the maximum displacement of clay will be less than that of PET (7.221e-01<1.451e+01 mm).

Graphics 1 and 2 reflect the results obtained from the finite element method in figures 3, 4, 5 and 6.

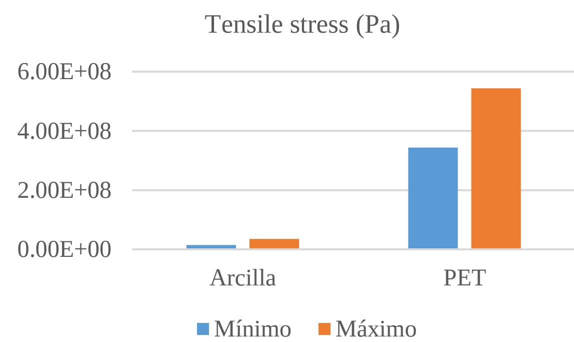

Graphic 1 Tensile stress difference (Pa) between the clay brick and the PET brick
Source: Own elaboration

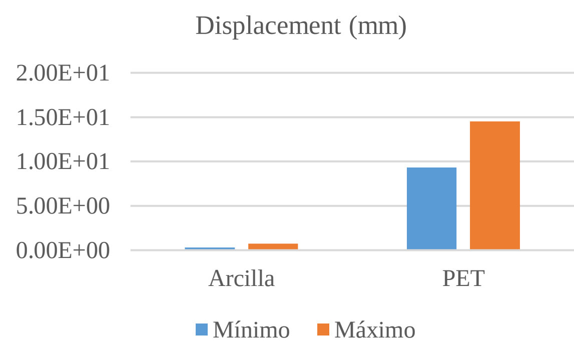

Graphic 2 Difference in displacement (Pa) between the clay brick and the PET brick
Source: Own elaboration

Conclusions

Within the mechanical analysis, the PET brick has better mechanical behaviour in compression than a clay brick, even though its dimensions are smaller than those of conventional bricks, making this material a possible input for the manufacture of bricks, and thus build quality internal dividing walls, as long as a good process of transformation of PET bricks is carried out and these are approved by the standardised tests.

To have a better validation of the mechanical behaviour for future works, flexural and water absorption tests can be used.

Given that PET is one of the most widely used waste plastics because it is recyclable, it is determined that this possible application can favour the care of the environment.

References

[1]. Nudelman, N. (2004). Química sustentable. Argentina: Universidad Nacional del Litoral. Recuperado de https://books.google.com.mx/books?id=DkQnfw1MuyUC&pg=PA105&dq=Su+incineraci%C3%B3n+puede+generar+gases+t%C3%B3xicos+y,+por+lo+tanto,+m%C3%A1s+contaminaci%C3%B3n&hl=es&sa=X&ved=2ahUKEwi82YGb9qPsAhUFi6wKHfA_BU8Q6AEwAHoECAUQAg#v=onepage&q=Su%20incineraci%C3%B3n%20puede%20generar%20gases%20t%C3%B3xicos%20y%2C%20por%20lo%20tanto%2C%20m%C3%A1s%20contaminaci%C3%B3n&f=false

[2]. Menashev, R. (2018). Mampostería de ladrillos. Aparejo escocés. Rusia: Litres. Recuperado de https://books.google.com.mx/books?id=nQBPDwAAQBAJ&pg=PT3&dq=Las+filas+de+ladrillos,+llamados+cursos,+se+encuentran+una+sobre+otra&hl=es&sa=X&ved=2ahUKEwiFl8Sk6JnsAhVCIqwKHfKvCJEQ6AEwAHoECAYQAg#v=onepage&q=Las%20filas%20de%20ladrillos%2C%20llamados%20cursos%2C%20se%20encuentran%20una%20sobre%20otra&f=false

[3]. Collado Trabanco, P. (2005). Control de ejecución de tabiquerías y cerramientos. España: Lex Nova, S.A. Recuperado de https://books.google.com.mx/books?id=N8IT-nhKapsC&pg=PA50&dq=qu%C3%A9+son+los+ladrillos&hl=es&sa=X&ved=2ahUKEwiCiIPIhJrsAhUFU80KHQwXCHkQ6AEwAXoECAMQAg#v=onepage&q=qu%C3%A9%20son%20los%20ladrillos&f=false

[4]. De Solminihac, H. & Thenoux, G. (2011). Procesos y térnicas de construcción. 5a Edición. Chile: Alfaomega u.c. de Chile Recuperado de https://books.google.com.mx/books?id=sM0oCAAAQBAJ&pg=PA331&dq=propiedades+mec%C3%A1nicas+de+los+ladrillos+de+arcilla&hl=es&sa=X&ved=2ahUKEwi_5-KhiovtAhVCWs0KHZnAAz0Q6AEwA3oECAUQAg#v=onepage&q=propiedades%20mec%C3%A1nicas%20de%20los%20ladrillos%20de%20arcilla&f=false

[5]. N-CTM-2-01-001/02. (2012). México: SCT. Recuperado de https://normas.imt.mx/normativa/N-CMT-2-01-001-02.pdf

[6]. Mehrdad, H. & Mehdizadeh Saradj, F. (2014). Persian Architectural Heritage: Structure. Southampton: WITPRESS. Recuperado de https://books.google.com.mx/books?id=9-kKAwAAQBAJ&pg=PA25&dq=mechanical+properties+of+clay+bricks&hl=es&sa=X&ved=2ahUKEwjFjpiMor_3AhW_JUQIHQoWD8E4ChDoAXoECAkQAg#v=onepage&q&f=false

[7]. Camacho, G. (2020). Resistencia de materiales: determinación de la resistencia a la flexión de ladrillos. Bolivia: Universidad Privada del Valle. Recuperado de https://www.studocu.com/bo/document/universidad-privada-del-valle/resistencia-de-materiales/laboratorio-de-resistencia-no7-en-grupo-medina-fernandez-ariel/10398634

[8]. Berreta, H., Gatani, M., Gaggino, R. & Argüelo, R. (2008). Ladrillos de plástico reciclado. Una propuesta ecológica para la vivienda social. Argentina: CEVE. Recuperado de https://books.google.com.mx/books?id=HbX-2l3nNisC&printsec=frontcover&dq=ventajas+y+desventajas+de+los+ecoladrillos&hl=es&sa=X&ved=2ahUKEwj7_aOwyp7sAhVJPK0KHeWFAFkQ6AEwAXoECAEQAg#v=onepage&q&f=false

ISSN: 2410-3438

[9]. Besednjak Dietrich, A. (2005). Materiales compuestos. Procesos de fabricación de embarcaciones. Barcelona: Universitat Politécnica de Catalunya, S.L. Recuperado de https://books.google.com.mx/books?id=gMSg5rURr6sC&pg=PA20&dq=clasificaci%C3%B3n+de+los+pol%C3%ADmeros&hl=es&sa=X&ved=2ahUKEwilyuq-

[10]. Kalpakjian, S. & Schmid, S. R. (2002). Manufactura, Ingeniería y tecnología. México: Prentice Hall. Recuperado de https://books.google.com.co/books?id=gilYI9_KKAoC&printsec=frontcover#v=onepage&q&f=false

[11]. Cabildo Miranda, M. et. al (2008). Reciclado y tratamiento de residuos. España: UNED. Recuperado de https://books.google.com.mx/books?id=jXEFxC3GiGQC&pg=PT277&dq=importancia+del+reciclaje+de+pl%C3%A1sticos&hl=es&sa=X&ved=2ahUKEwjr3ufqpK3sAhUVHM0KHRwoCDQ4ChDoATAAegQIBRAC#v=onepage&q=importancia%20del%20reciclaje%20de%20pl%C3%A1sticos&f=false

[12]. Beltrán Villavicencio, A. et. al. (2022). El reciclaje de los plásticos. Azcapotzalco: anipac. Recuperado de http://biblioteca.anipac.mx/wp-content/uploads/2016/10/0047_El_Reciclaje_de_los_Plasticos.pdf

[13]. Flores Ramírez, R. N. (2019). Ladrillos de plástico reciclado para mampostería no portante. Ecuador: Universidad Católica de Cuenca. Recuperado de http://186.5.103.99/handle/reducacue/8297

[14]. Campos Barboza, K.L. et. al. (2019). Diseño del proceso de producción de ladrillos basados en plástico reciclado. Perú: Universidad de Piura. Recuperado de https://pirhua.udep.edu.pe/bitstream/handle/11042/4292/PYT_Informe_Final_Proyecto_Ladrillos_PET.pdf?sequence=1&isAllowed=y

[15]. Díaz del Castillo Rodríguez, F. (2018). Método del elemento finito y AutoFEM. México: UNAM Cuautitlán. Recuperado de http://olimpia.cuautitlan2.unam.mx/pagina_ingenieria/mecanica/mat/mat_mec/m1/Elemento_finito_Autofem.pdf

[16]. Carrillo Julián, Alcocer Sergio y Aperador William. Propiedades mecánicas del concreto para viviendas de bajo costo, Ingeniería, Investigación y Tecnología, Volumen 14, Issue 2, Abril - Junio 2013, Pages 285-298. Recuperado de https://www.redalyc.org/pdf/404/40426155011.pdf.

Article **Journal of Quantitative and Statistical Analysis**
June 2022, Vol.9 No.24 15-22

Thermodynamic analysis of a Stirling cycle with nuclear heat source for aerospace applications

Análisis termodinámico de un ciclo Stirling con fuente de calor nuclear para aplicaciones aeroespaciales

DÍAZ-ESPINOZA, Gerardo†*, GALLARDO-VILLARREAL, José Manuel and VALLE-HERNÁNDEZ, Julio

Universidad Politécnica Metropolitana de Hidalgo, Mexico.
Universidad Autónoma del Estado de Hidalgo, Mexico.

ID 1st Author: *Gerardo, Díaz-Espinoza* / **ORC ID:** 0000-0003-1293-0275, **CVU CONACYT ID:** 926199

ID 1st Co-author: *José Manuel, Gallardo-Villarreal* / **ORC ID:** 0000-0002-7578-7229, **CVU CONACYT ID:**366394

ID 2nd Co-author: *Julio, Valle-Hernández* / **ORC ID:** 0000-0001-8957-0066, **CVU CONACYT ID:** 210743

DOI: 10.35429/JQSA.202.24.9.15.22 Received January 20, 2022; Accepted June 30, 2022

Abstract

The main requirement for the development of aerospace missions is the energy supply, for example, 10 kWe would be required for the day and 9 kWe for the night during the first phase of construction of a human settlement on the moon. To satisfy the energy demand, it was proposed the use of heat due to a nuclear fission reaction, coupled to a Stirling engine as a dynamic power converter. The Stirling engine is used since it has less mass, a smaller heat sink area and a longer useful life compared to another type of power converter, thus being the most suitable for coupling with the Optimized Evolutionary Growth Lunar nuclear reactor, which will be the thermal power source of the electrical power generation system presented in this article. In this article, it is shown the thermodynamic analysis that involves the transport of heat from the nuclear reactor to helium as the working fluid of the dynamic power converter. The initial parameters are obtained for the analysis: temperature, pressures and volumes, which will allow us to carry out the mathematical modeling of the Stirling Method (Ideal). As results, a comparison is presented between the variations of proposed parameters with the purpose of determining the behavior of the useful work and the electrical power in the system, evaluating the compression ratio, the angular velocity and the initial pressure.

Stirling engine, Nuclear reactor, Thermodynamic analysis

Resumen

El principal requerimiento para el desarrollo de misiones aeroespaciales es el suministro energético, por ejemplo, se requeriría 10 kWe para el día y 9 kWe para la noche durante la primera fase de construcción de un asentamiento humano en la luna. Para satisfacer la demanda energética se propone el aprovechamiento del calor debido a una reacción nuclear de fisión, acoplada a un motor Stirling como conversor de potencia dinámica. Se utiliza al motor Stirling ya que tiene menor masa, menor área de disipador de calor y mayor vida útil en comparativa con otro tipo de conversor de potencia, siendo así el más apto para el acoplamiento con el reactor nuclear Lunar de Crecimiento Evolutivo Optimizado, el cual será la fuente de potencia térmica del sistema de generación de potencia eléctrica presentado en este artículo. En este trabajo se presenta el análisis termodinámico que involucra el transporte de calor del reactor nuclear al helio como fluido de trabajo del convertidor de potencia dinámica. Para el análisis se obtienen los parámetros iniciales: temperatura, presiones y volúmenes, los cuales nos permitirán realizar el modelado matemático el Método Stirling (Ideal). Como resultados se presenta una comparativa entre la variación de parámetros propuestos, con la finalidad de determinar el comportamiento del trabajo útil y la potencia eléctrica en el sistema, evaluando la relación de compresión, la velocidad angular y la presión inicial.

Motor Stirling, Reactor nuclear, Análisis termodinámico

Citation: DÍAZ-ESPINOZA, Gerardo, GALLARDO-VILLARREAL, José Manuel and VALLE-HERNÁNDEZ, Julio. Thermodynamic analysis of a Stirling cycle with nuclear heat source for aerospace applications. Journal of Quantitative and Statistical Analysis. 2022. 9-24:15-22.

* Correspondence to the Author (E-mail: 213220016@upmh.edu.mx)
† Researcher contributing as first Author.

Introduction

NASA is developing different missions that involve three space applications: Rovers and Satellites, Propulsion, and Settlement. This last application suffers from the problem of how electrical power is supplied, an example of this is the energy consumption demanded for the first stage of lunar habitation established in Power System Requirements and Definition for Lunar and Mars Outposts (I), which is 5-6 kilowatts electric (kWe) (I).

In recent years, the use of solar energy has been implemented as an electrical power supply, however, the use of these mechanisms has disadvantages due to the long duration of the night (14 Earth days) involving the solar cells do not work during that period of time, likewise, during the day, the system is subjected to a large amount of heat causing the efficiency decreases.

It begins to analyse the advantages of using a nuclear source as a thermal power supply, one of them is to provide constant energy, which is a necessity for human life support systems, rover recharging and resource extraction, unlike solar energy which requires the use of energy storage devices increasing unwanted mass to the system (I).

Therefore, the selection of a nuclear reactor with characteristics concerning the feasibility of use on the moon has been made, in this case, the Lunar Evolutionary Growth Optimised (LEGO)(II) nuclear reactor represents a system capable of providing an initial supply of useful thermal power for power conversion, reaching the electrical power required to satisfy the energy need.

The thermal power supplied by the LEGO nuclear reactor is 24 kWt (II), using Uranium Dioxide as fuel and implementing metallic liquid sodium as coolant, transporting the heat to a first exchanger where potassium is located, generating a phase change from liquid to vapour that will transport the heat to the power converter.

It has been decided to implement a dynamic power converter for heat utilisation, involving high efficiency, lower mass for transportation and sufficient power supply required, being the Stirling engine the most viable system compared to other types of converters.

Therefore, the contribution of this article is to perform the thermodynamic analysis of the Stirling engine to have an approach to the behaviour of the cycle in ideal and ideal geometric conditions, being the basis of a project in which real conditions of heat transfer and behaviour of working fluids in the coupling of the nucleoelectric system will be determined.

Then, the sections of this work are presented. For the first section, the initial parameters of the Stirling engine system (XI) are determined.

Finally, the modelling of the Stirling engine is established, based on the First Order Model corresponding to the Ideal Stirling Cycle where the initial parameters will be used to carry out the analysis and verification of all the characteristics involved in obtaining the electrical power.

Methodology

The following are the procedures to be used to carry out the research presented (Fig. 1).

I. Define the initial temperature of the working fluid in the expansion zone of the engine due to the thermal power released by the nuclear reactor.

II. Obtain initial parameters that will be used in the modelling of the Stirling engine.

III. To analyse the thermodynamic cycle for a Stirling engine based on the Carnot Cycle, generating the first order model Ideal Stirling Model.

IV. To evaluate the electrical power and efficiency of the cycle by comparing the values proposed in the model.

ISSN: 2410-3438

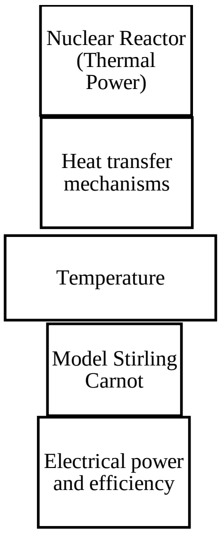

Figure 1 Development of the methodology

Modelling Considerations

Thermal Power and Heat Transfer

The Optimised Evolutionary Growth Lunar nuclear reactor is proposed for this analysis as the heat source for this system, its thermal power behaviour was the reference for this article, using 24 kWt as the constant value in the system to obtain the temperature of the helium as the working fluid in the Stirling Cycle (II).

Ideal conditions were used to determine the initial parameters in the system, with conduction and convection heat transfer mechanisms being the means to determine these values.

$$Q = \frac{2\pi Lk(T_{PI}-T_{PE})}{\ln\left(\frac{r2}{r1}\right)} \tag{1}$$

$$Q = 2\pi r_1 Lh(T_{PE} - T_\alpha) \tag{2}$$

$$Q = mC_p\left(\frac{dT_\alpha}{dt}\right) \tag{3}$$

Where k is the value of the conductivity of the material in the system, A=2πrL the respective area in each section, Tpi the initial reactor temperature, Tpe the external wall temperature, Tα the fluid temperature, m the total mass of the system, h the convective heat transfer coefficient and Cp the specific heat (VII).

The idealisation of the system is schematized below.

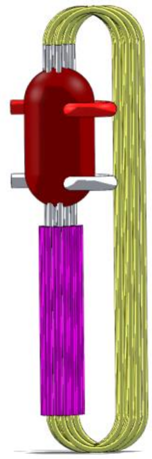

Figure 2 Idealisation of the coupled system

Fig 2 shows the section of the lunar nuclear reactor denoted by the pink colour, the high conductivity piping in white and yellow, the first heat exchanger where the potassium is stored in red.

Sodium as the main working fluid transports the heat through the nuclear reactor, then the thermal power is delivered to the first heat exchanger where potassium is stored.

Finally, the helium in the Stirling engine section receives the heat transported by the potassium due to the first heat exchanger, being this temperature the one used in the cycle to be developed (II).

The selection of 4 proposed parameters is included in which, as first parameter, is the initial pressure that will establish the first process due to the obtaining of the specific volume of the thermodynamic cycle respectively.

As a second parameter, the compression ratio is selected, which based on the Stirling Engine Design Manual (X) shows that there can be a variation of this ratio in an interval of 1.8 to 3 for a Stirling engine, being the optimum values to determine the change in the volume in the compression zone.

Subsequently, the angular velocity that will be included in obtaining the resulting mechanical power in the system will be selected and a comparison will be made to determine the optimum values (IX).

Obtaining the initial cycle parameters

The proposed parameters in table 1 are:

Parameters proposed	
Initial Pressure (kPa)	200
Compression Ratio	1.8
Angular velocity (rpm)	1500
Geometric Volume (m^3)	0.009

Table 1 Proposed parameters for Stirling engine modelling

The ideal gas characteristics are also established to determine the initial working parameters of the Stirling cycle, including equation (1), (2) and (3) to determine the value of the working fluid temperature due to the thermal power of the reactor (Table 2). (Table 2)

$\dot{Q}$ (kWt)	T_1 (K)	P_1 (kPa)	$V_1\left(\frac{m^3}{kg}\right)$	T_3 (K)
24	973	200	10.07	600

Table 2 Initial parameters for Stirling engine modelling

As shown in equation (4), based on the geometric volume parameter, the total mass in the system was obtained by referring to the specific volume of expansion, the largest area.

$$m = \frac{V_g}{V_e} = 0.00049\, kg \quad (4)$$

Modelling of the Stirling engine

For the modelling of the Stirling engine, the geometrical configuration type Beta was considered, where the cycle is driven by a piston and a displacer operating concentrically in the same cylinder (X).

Taking into account these characteristics, this type of engine was considered for its aerospace application, since, through an arrangement to the mechanical system, which interconnects the expansion and compression section, it could be hermetically sealed avoiding the leakage of the working fluid, being this a desirable feature for an implementation in the lunar environment (V).

The working fluid in this system is helium due to its low molecular weight and high thermal conductivity compared to other working fluids used in this system. other working fluids used in this type of configuration (IV).

As a first approach to the mathematical and thermodynamic model of the Stirling engine, the ideal modelling is established based on the Carnot cycle made up of the four processes shown in table 3.

Process	
1-2	Isothermal Expansion
2-3	Isothermal Expansion
3-4	Isothermal Compression
4-1	Isentropic Compression

Table 3 Thermodynamic processes for Carnot method

In contrast to the Carnot modelling, the Ideal Stirling model replaces the isentropic processes with two regeneration processes, in which heat is transferred to a thermal energy storage system and subsequently delivered to another process in the system.

Ideal Stirling model

The modelling of the Ideal Stirling Cycle is described in Table 4, and allows us to determine the thermodynamic behaviour of the Stirling engine, based on the law of conservation of mass, considering ideal conditions without losses and reversible.

Process	
1-2	Isothermal Expansion
2-3	Regenerative Cooling
3-4	Isothermal Compression
4-1	Regenerative Heating

Table 4 Thermodynamic processes for ideal Stirling method

Three main equations have been established to carry out the modelling of the Ideal Stirling cycle, the first equation is the one corresponding to the law of conservation of energy shown in equation (5) which establishes the change in internal energy based on heat and work in the whole system (VII).

$$\Delta U = Q - W \quad (5)$$

The second equation of the model corresponds to the work in a process of isothermal compression or expansion, as shown in the following equation:

$$W = \int pdV \quad (6)$$

ISSN: 2410-3438

Finally, the third equation used corresponds to the ideal gas equation (7), which is useful to determine the changes in specific volume, pressure and temperature, respectively.

$$PV = mRT \quad (7)$$

With these three equations, the values of each process of the Thermodynamic Cycle are determined.

Stirling Thermodynamic Cycle

a) Isothermal Expansion

For the isothermal expansion process, there is no variation in the internal energy because the temperature remains constant as shown in:

$$\Delta U_{1-2} = mC_v(T_2 - T_1) = 0, T_2 = T_1 \quad (8)$$

C_v being the specific heat at constant specific volume, m the total mass in the system T_2 the temperature in the compression zone and T_1 the temperature in the expansion zone.

It is also implied that the gas does work and therefore has to absorb an equal amount of energy from the heat supply to keep its temperature constant.

$$Q_{1-2} = W_{1-2} = mRT_e \ln\left(\frac{V_1}{V_2}\right) \quad (9)$$

where m is the mass in the system, R is the ideal gas constant, V_1 is the specific volume in the compression zone and V_2 is the specific volume in the expansion zone.

b) Regenerative Cooling

In the regenerative cooling section, it is stated that there is no work in this process because the specific volume in the process remains constant.

$$W_{2-3} = mRT_c \ln\left(\frac{V_2}{V_3}\right) = 0 , V_2 = V_3 \quad (10)$$

is shown as a process in which the gas gives up heat, decreasing its internal energy and therefore its temperature decreases.

$$Q_{2-3} = \Delta U_{2-3} = mC_v(T_3 - T_2) \quad (11)$$

c) Isothermal Compression

Being the process where the gas is compressed at the constant temperature of the compression zone, from the specific volume V_2 to the final specific volume V_1.

$$\Delta U_{3-4} = mC_v(T_4 - T_3) = 0, T_4 = T_3 \quad (12)$$

The work for this process is due to the low-pressure gas, being less than during the expansion process.

$$Q_{3-4} = W_{3-4} = mRT_e \ln\left(\frac{V_3}{V_4}\right) \quad (12)$$

It must supply the same amount of heat to keep the temperature constant compared to the expansion section.

d) Regenerative Heating

The behaviour in this process is at constant volume, causing zero work in this section because of

$$W_{4-1} = mRT_c \ln\left(\frac{V_1}{V_4}\right) = 0 \quad , V_1 = V_4 \quad (13)$$

For the heat of temperature change at constant specific volume, the increase in internal energy is established, therefore:

$$Q_{4-1} = \Delta U_{4-1} = mC_v(T_1 - T_4) \quad (14)$$

Making use of the values obtained in each process, we proceed to determine the efficiency and mechanical power based on the following equations:

$$\eta = \frac{W_T}{Q_e} \quad (15)$$

W_T being the network in the variation of the expansion and compression work, and Q_e the heat in the compression zone.

$$Pot = \frac{W_T * \dot{n}}{n_{rev}} \quad (16)$$

Where $\dot{n}$ is the angular velocity established at the beginning of this article and n_rev is the number of revolutions per unit cycle, for the case of the Stirling engine the value is 1 rev/cycle (VII).

ISSN: 2410-3438

Results and discussion

In the pressure-volume diagram in Graph 1, the four processes corresponding to the thermodynamic cycle can be observed.

For section 1-2, the decrease of the initial pressure (Table 1) is noted, reaching a point where the specific volume will have no variation.

When it reaches 111 kPa, the following process takes place, the specific volume remains constant while the temperature decreases, this is due to regenerative cooling, where the regenerator absorbs heat and stores it.

When the minimum pressure is reached, the compression process takes place due to the regression of the piston in the expansion zone, so the specific volume decreases and the pressure increases.

Finally, when the maximum specific volume point is reached, heating occurs due to the influence of the regenerator, which delivers the heat absorbed in the process 2-3, generating an increase in temperature, which leads to the restart of the cycle.

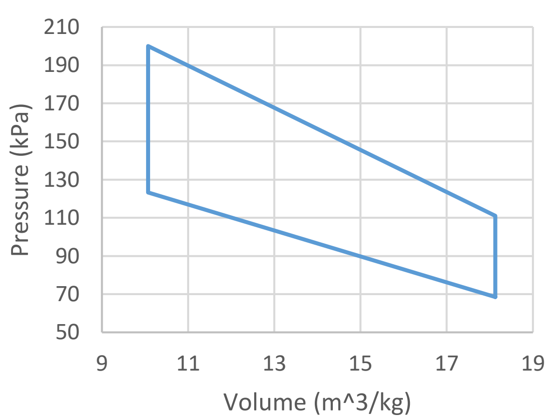

Graphic 1 Ideal PV Diagram

For Graphic 2, the bounded area represents the resulting heat in the system with respect to the entropy change, observing in the cooling process a decrease in temperature and in the regenerative heating of the fluid an increase.

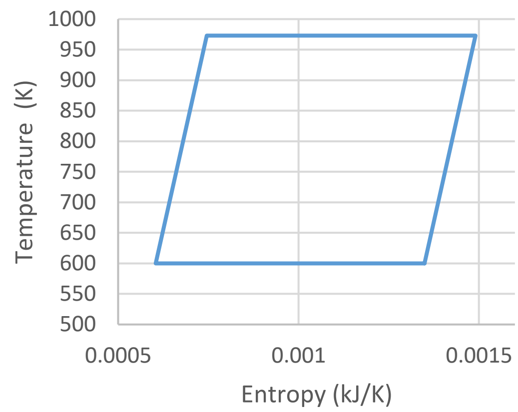

Graphic 2 Ideal TS Diagram

In Graphic 3, it can be seen that the power required by the Lunar Evolutionary Growth Reactor has been reached, being 5.63 kWe, which allows us to verify that the mathematical modelling is correct (II).

By the variation in the compression ratio that, as a respective increase, the power also increases, however, increasing the compression ratio causes the decrease in power, therefore, it was proposed to fix the value of compression ratio and make the variation in other parameters.

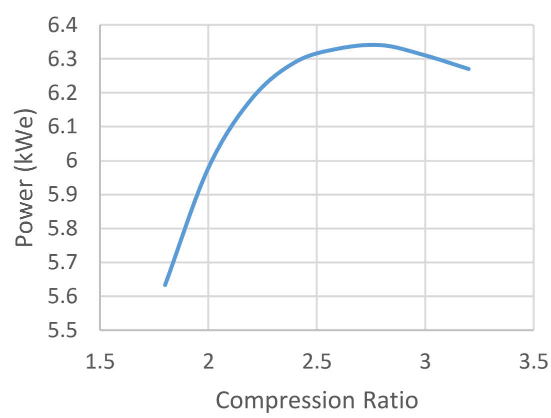

Graphic 3 Compression Ratio Variation

For Graphic 4, the variation in the value of the pressure in the expansion section was carried out, observing the considerable increase in the useful work, being a 33% increase by increasing 1 atm, however, it has been decided that the use of the working fluid is at low pressure due to present structural advantages in terms of chemical compatibility with the material and decreasing the possible leaks in the system being more manageable for the user.

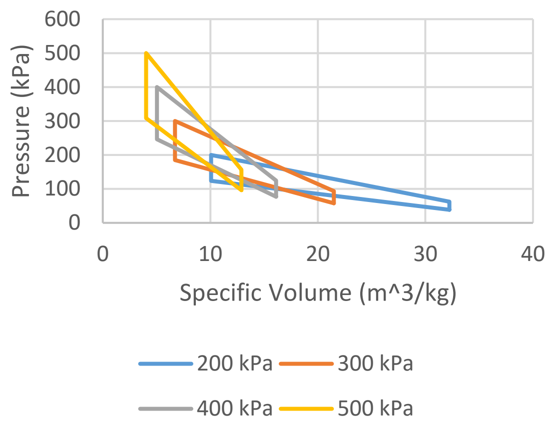

Graphic 4 Expansion zone pressure variation

According to Graphic 3, it is established that if there is an increase in the compression ratio there will be an increase in the power delivered by the system, however, it is determined in Graphic 5 that, if the compression ratio continues to increase, the performance of the system decreases, so it is necessary to establish an optimum point by limiting the increase in the expansion volume to 2.8.

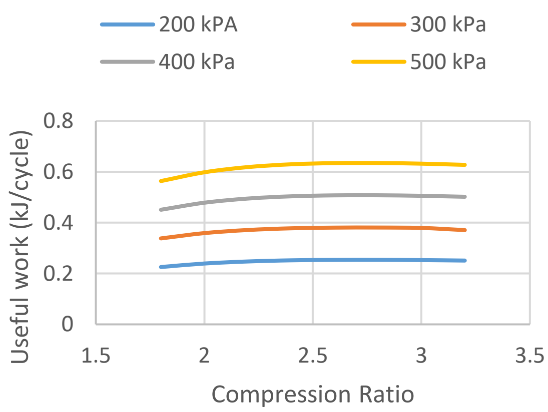

Graphic 5 Variation of useful work due to compression ratio

The variation of the useful work at different pressures was reviewed, as it can be observed, the increase in the initial pressure causes an increase in the value of the useful work, however, the variation of the compression ratio was maintained, causing the same behaviour of performance decrease.

Conclusions

The verification of this model was based on the results established in the article A Basic LEGO Reactor Design for the Provision of Lunar Surface Power. United States (II), as it provides an electrical power supplied by the nuclear reactor of 5.63kWe.

Based on the characteristics of high efficiency, structural advantages, size, weight, lifetime and use of a regenerative system, the Stirling Cycle engine was determined to be the most viable power converter for the problem set out in this paper.

The optimal results of system behaviour with the characteristics of the initial parameters proposed were arrived at through mathematical modelling.

Taking into account that the electrical power requirements are not so high, it was decided to maintain a relatively low angular velocity for this system based on the analysis of the results in section 5 of this article.

However, it was observed that increasing the compression ratio at a certain point the power starts to decrease presenting low efficiency, which allows us to analyse the optimal compression ratio value for the system.

The implementation of a Thermodynamic Stirling Cycle showed the behaviour that the proposed variables can be modified according to the user's needs.

Finally, reference is made to the previous results being the optimal system parameters for the need of this article; for future projects they will be taken as a basis to develop a real geometrical analysis and the thermo-hydraulic modelling of certain sections of the above mentioned nuclear power system (IV).

Funding

The present work has been funded by CONACYT Grant Number 926199.

References

1. Cataldo, Robert L. (1993) Power Requirements for the First Lunar Outpost (FLO). Lewis Research Center. Cleveland, Ohio. NASA. https://ntrs.nasa.gov/api/citations/19930006334/downloads/19930006334.pdf

2. Bess, John Darrell. A Basic LEGO Reactor Design for the Provision of Lunar Surface Power. United States. (INL/CON--08-14353) https://inldigitallibrary.inl.gov/sites/sti/sti/4010758.pdf

ISSN: 2410-3438

3. Tournier, Jean-Michel & El-Genk, Mohamed. (2005). Liquid Metal Heat Pipes Radiator for Space Nuclear Reactor Power Systems. Collection of Technical Papers - 3rd International Energy Conversion Engineering Conference. 3. DOI:10.2514/6.2005-5701. https://www.researchgate.net/publication/268572847_Liquid_Metal_Heat_Pipes_Radiator_for_Space_Nuclear_Reactor_Power_Systems

4. Mohamed S. El-Genka (2011) USES OF LIQUID-METAL AND WATER HEAT PIPES IN SPACE REACTOR POWER SYSTEMS. Institute For Space and Nuclear Power Studies, Chemical & Nuclear Engineering Dept., University Of New Mexico, Albuquerque, NM 87131, USA. DOI: 10.5098/Fhp.V2.1.3002. https://www.researchgate.net/publication/268572847_Liquid_Metal_Heat_Pipes_Radiator_for_Space_Nuclear_Reactor_Power_Systems

5. Ehud Greenspan (2008) Solid-Core Heat-Pipe Nuclear Battery Type Reactor. University of California Department of Nuclear Engineering Berkeley. DE-FC07-05ID14706 https://www.osti.gov/servlets/purl/940911

6. G. Sofer. (1961) Conceptual Design And Economic Evaluation Of A Steam-cooled Fast Breeder Reactor. United States Atomic Energy Commission. NSA-15-021888 https://www.osti.gov/biblio/4769045-evaluation-steam-cooled-fast-breeder-reactors

7. Cengel, Yunus A. (2004) TRANSFERENCIA DE CALOR Y MASA. Fundamentos y aplicaciones. University of Nevada, Reno. https://www.academia.edu/12140362/Transferencia_de_Calor_y_Masa_4ta_ed_Yunus_Cengel

8. Urieli, Israel (1977) A Compute Simulation of Stirling Cycle Machines. Faculty of Engineering, University of the Witmatersrand, Johannesburg. https://www.ohio.edu/mechanical-faculty/urieli/Izzi_PhD_thesis.pdf

9. Mason, Lee S. (2001) A Comparison of Brayton and Stirling Space Nuclear Power Systems for Power Levels from 1 Kilowatt to 10 Megawatts. Gleen Research Center, Cleveland, Ohio. https://ntrs.nasa.gov/api/citations/20010016863/downloads/20010016863.pdf DOI:10.1063/1.2169203

10. Martini, William (1983) Stirling Engine Design Manual. Lewis Research Center. U.S. Department of Energy. https://ntrs.nasa.gov/api/citations/19830022057/downloads/19830022057.pdf.

ISSN: 2410-3438

Article **Journal of Quantitative and Statistical Analysis**
June 2022, Vol.9 No.24 23-31

Brake systems tribological analysis and their evolution in sustainable characterization

Análisis tribológico de sistemas de frenos y su evolución en la caracterización sustentable

LAGOS-LÓPEZ, Lorena†, CRUZ-GOMEZ, Marco Antonio*, MEJÍA-PÉREZ, José Alfredo and ESPINOSA-CARRASCO, María del Rosario

Benemérita Universidad Autónoma de Puebla; Faculty of Engineering, Tribology and Transportation Group, Academic Body 189 (Disaster Prevention and Sustainable Development, Tribology, BUAP), Graduate Building, First Level, Cubicle No. 16, Blvd. Valsequillo esq. Av. San Claudio, Ciudad Universitaria, Col. San Manuel, CP. 72570, Puebla Mexico.

ID 1st Author: *Lorena, Lagos-López* / **ORC ID:** 0000-0002-7865-6443, **Researcher ID Thomson:** AFR-3376-2022, **CVU CONACIT ID:** 1190369

ID 1st Co-author: *Marco Antonio, Cruz-Gómez* **/ ORC ID**: 0000-0003-1091-8133, **Researcher ID Thomson**: S-3098-2018, **CVU CONACYT ID**: 349626

ID 2nd Co-author: *José Alfredo, Mejía-Pérez* / **ORC ID:** 0000-0002-4090-8828, **Researcher ID Thomson:** G-3354-2019

ID 3rd Co-author: *María del Rosario, Espinosa-Carrasco* / **ORC ID:** 0000-0002-5094-2800, **Researcher ID Thomson:** AAP-2965-2020, **CVU CONACYT ID:** 1018747

DOI: 10.35429/JQSA.2022.24.9.23.31 Received January 25, 2022; Accepted June 30, 2022

Abstract

This research aimed to analyze the different brake systems using tribology as a tool for the optimization of controlled systems. Automotive braking systems in high-tech technology were analyzed to identify the variables involved and relate them to the results of the different tribological studies. Traditional braking systems were compared with respect to the regenerative ones used in high-end hybrid and electric cars, in order to identify the technologies applied in tribological systems and their evolution. The variables analyzed were force, contact area, friction coefficient, force cyclical variation, rpm, time, acoustic emission, sliding speed, torque, temperature, and surface misalignment, among others. The results of the different case studies determined that regenerative brake systems are prototypes in continuous sustainable evolution and tribology, together with electronics, contributes with analyzes to achieve more precise controlled systems.

Sustainable braking technology, Tribological studies, Regenerative brake systems

Resumen

Esta investigación tuvo como objetivo analizar los diferentes sistemas de frenos utilizando como herramienta la tribología para la optimización de sistemas controlados. Sistemas de frenado en automóviles de alta vanguardia tecnológica fueron analizados para identificar las variables involucradas y relacionarlas con los resultados de los diferentes estudios tribológicos. Sistemas de frenado tradicionales fueron confrontados con respecto a los regenerativos utilizados en autos híbridos y eléctricos de alta gama, con la finalidad de identificar las tecnologías aplicadas en sistemas tribológicos y su evolución. Las variables analizadas fueron fuerza, área de contacto, coeficiente de fricción, variación cíclica de la fuerza, rpm, tiempo, emisión acústica, velocidad de deslizamiento, torque, temperatura, desalineación de la superficie entre otras. Los resultados de los diferentes casos de estudio determinaron que los sistemas de frenos regenerativos son prototipos en evolución continua sustentable y la tribología en conjunto con la electrónica contribuyen con análisis para lograr sistemas controlados de mayor precisión.

Tecnología de frenado sustentable, Estudios tribológicos, Sistemas de frenos regenerativos

Citation: LAGOS-LÓPEZ, Lorena, CRUZ-GOMEZ, Marco Antonio, MEJÍA-PÉREZ, José Alfredo and ESPINOSA-CARRASCO, María del Rosario. Brake systems tribological analysis and their evolution in sustainable characterization. Journal of Quantitative and Statistical Analysis. 2022. 9-24:23-31.

* Correspondence of the Author (E-mail: lorena.lagos@alumno.buap.mx)
† Researcher contributing as first Author.

Introduction

Tribology analyzes the quantification of wear phenomena at the macro, micro, and nanoscale levels such as abrasion, adhesion, sliding, cracking, fatigue, rolling contact, delamination, cavitation, impact, corrosion, and erosion, or a combination of these. The metrology of the wear types in cyclic behaviors identifies the critical factors that will be standardized under ISO 25178 to understand, predict and control the problem. The primary objective of tribology is to optimize the design of a component or assembly to propose a surface finishing process, coating formulation, or lubrication method. (Lugt, 2016; Stoica & Tudor, 2015). The tribology objectives is to minimize wear, optimizing friction as a function of temperature in the contact area in brakes, clutches, and tires. (Benalcázar & Gabriela, 2022; Li et al., 2018; Syahir et al., 2017).

Braking is related to the wear phenomena due to abrasion, sliding, and adhesion, mainly causing an increase in temperature that is transmitted to the entire system, generating the transformation of energy between a fixed part "caliper" and a rotating "disc". When we activate the brake pedal, it is pressurized by a hydraulic circuit that moves the brake pads, exerting pressure on the disc until it locks. The pads must withstand high temperatures without excessive wear, but with a friction coefficient sufficient to achieve the braking conditions required in the vehicle by the user or by an automated system that help the vehicle detect objects that could potentially affect its trajectory. (Zhao et al., 2018)

The friction coefficient of the pad material must be as stable as possible at different speeds, pressures, and temperatures so that the driver or the automatic braking system can anticipate the vehicle's reaction to different operating or environmental conditions. (Benedetti et al., 2017; Fernandes, 2016). Braking systems were classified into; hydraulic and combined. The hydraulic systems can be divided into three groups; disc, drum, and hand. Combined braking systems were; hydraulic and electric – hydraulic. Combined electric-hydraulic systems were called “regenerative”.

The handbrake was only applied to the rear tires while in some cases the braking systems may be mixed on one mobile depending on the drive wheels number (directly connected to the transmission). In the case of regenerative braking systems, they can only be applied to systems directly coupled to the transmission. (Bauer, 2019; Fernandes, 2016)

Figure 1 Regenerative braking system
Source: Fernandes M. (2016)

Regenerative brakes are different from friction brakes, in that the electric motor works in reverse when the driver hits the brakes. The vehicle slows down and, at the same time, electricity was generated and stored in the battery for reuse. With traditional braking systems, this energy is lost in the form of heat, but in regenerative braking systems, the energy was used, improving the energy efficiency of the vehicle and extending the useful life of the braking system due to less wear. (Champi & Abel, 2022; Tormos et al., 2017)

In combined brake systems, the car's computer determines when to activate the friction or regenerative braking system. A slight reduction in force on the brake pedal causes the vehicle's electronics to activate the regenerative brakes and place the motor in reverse to generate electrical energy that will be sent to the battery bank. On the contrary, if the vehicle needs to stop quickly to avoid a collision, only the conventional brakes will be applied to avoid damaging the regenerative systems, which depend entirely on the programmed logic of activation and deactivation of the electronic systems in the event of a vehicle operation. The user that develops in an environment. (Gong et al., 2015; Ma & Zhan, 2015).

These systems use many additional sensors to send signals to a central computer, which, under programmed logic, identifies in an algorithm the response that will be sent to the braking system according to the user's operating condition with its environment. The response of combined friction and regenerative braking system requires a feedback system in a closed-loop circuit. On the other hand, one of the drawbacks of these electronic systems are the environmental conditions, which can be unpredictable for the logical control system, such as snow, hydroplaning, pollutants, poor track conditions, and irregular soils such as dirt or roads in inappropriate conditions, among others, which, by not having the capacity to respond to adverse conditions, generates an arbitrary response within its possibilities that does not optimize the regenerative braking system. (Gong et al., 2015; Ma & Zhan, 2015).

Since we are talking about hybrid and electric vehicles, where efficiency is a priority, systems will always try to maximize the amount of braking torque provided by regeneration which is directly proportional to generator voltage feedback which was limited. by the speed at which the batteries can absorb energy and by the state of charge of the battery, (if it is fully charged it is not possible to store it. (Wicki & Erik, 2017)

The perfect brake pad in terms of friction performance, wear, noise, operating temperature, and costs have not been found to date, because the idealizations are: low speeds and pressures, decrease in settling time, and use of brake energy. dissipation friction, generation of maximum torque output, and no corrosion. (Mukoyama et al., 2017).

The closest modeling attempts are related to the generation of tribological banks, which base their designs on the analysis of experiments and the creation of feedback algorithms for the generation of software, where the choice of the system variables and their limit conditions allow a replica of real system scaling.

Obtaining high-precision data depends on the interfaces of the different sensing devices that deliver signal spectra that can be analyzed separately, but tribology establishes that as a critical point of analysis, the relationship between these to be interpreted and represent the scientific foundation in decision-making in engineering areas, to lay the foundations to generate new controlled technologies. (Kumar et al., 2018; Shababi et al., 2017)

The tribological properties during the braking phenomenon have an influence on the operation and its failures such as noise and vibrations that appear at very low sliding speeds for another phenomenon called sliding to occur, the static friction coefficient (μs) between two braking surfaces contact of the friction materials must be greater than the kinetic friction coefficient (μk). (Shababi et al., 2017 ; Zhang et al., 2016). The adhesion slip phenomenon generally appears at very low slip speeds as intermittence in the friction process caused by differences between the values of kinetic and static friction coefficients. This research analyzes the contributions of tribology in standard vs regenerative braking systems, showing the form of analysis based on test benches designed for the purpose to obtain controlled tests so that they can iterate these variables in electronic sensing models. to automate braking control systems in high-end electric cars.

Tribological analysis tests

Tribological tests of traditional friction braking systems, actuated by hydraulic systems, were analyzed by different authors, identifying the friction coefficient as a fundamental parameter based on the materials involved in the tests. (Shababi et al., 2017). All these study cases required control of different test variables such as force, contact area, friction coefficient, cyclical variation of force, rpm, time, acoustic emission, sliding speed, circular paths on the disk of contact, torque, temperature, surface misalignment, contacts, contaminated, dry and wet under different lubrication regimes among others.

The tests were carried out in different types of tribometers, both horizontal and vertical, with standardized tests that used the Pin on disc method under the ASTM G-99 standard. The objective of these tests was in all cases, to determine the behavior of different steel types in the manufacture of braking disc systems, as well as the proposal to use stainless steel to manufacture corrosion-free braking discs. On the other hand, the materials used in the manufacture of different brake pad types were used for the manufacture of bolts. These contacts were analyzed for their abrasive and adhesive wear behavior as a function of the variation of the aforementioned test variables to identify the optimization of test parameters in the different contact types, which optimized the coefficients of friction in the range of 0 – 3.

Most tests were carried out in the range of the following parameters: maximum sliding speed: 0.13 - 0.3 m/s, maximum contact pressure: 0.88 - 0.1 MPa, total sliding time: 2 - 300 s, disc mass : 0.167 - 0.3 g, specific heat for gray cast iron: 560 J / (kg K), angular speed 1 - 25 rad/s, normal load of (25, 50, 75, 100, 150, 200) N, speeds (20 , 40, 60, 80, 100) rpm, acoustic emission from 4 - 70 dB, braking contact temperature at different speeds; calculated at closed contact 100 - 1100 °C. (Huang et al. 2019; Nuñez & Andree, 2022; Shababi et al., 2017,)

The friction coefficient and the acoustic emission identified from several tests that when the load was increased the acoustic emission increased, in the last part of the tests in a cyclical way with only a few intermittences. For a better understanding of what was happening, they chose 10-s test periods to highlight the phenomenon. In these short-term tests, it was observed that the coefficient of friction and the acoustic emission between seconds 200 and 210 of the 300-s test, the disc makes a complete rotation every second, and the coefficient of friction presented the same evolution from one cycle to another. Therefore, it was decided to reduce the period to 2 s with the same test conditions, identifying that compared to the tests in which we do not have acoustic emission, there is a drop and sudden increases in the values of the coefficient of friction that was repeated every cycle with different amplitudes that were considered a slip period. (Kumar et al., 2018).

During this period just before the contact block, it was possible to identify that most of the energy is lost during stop-and-go driving, which is the energy absorption optimization period that we are looking for so that the regenerative brakes are more efficient. During the braking tests, it was identified that up to 80% of the energy could be lost in the stopping and starting phenomena where the temperature was measured by conduction because it is the method of greater precision and accuracy with economic instrumentation. Previous case studies have identified that regenerative braking can often retain nearly half of that lost energy that was converted to heat by closing the ignition. This energy can be transformed by regenerative systems into electrical energy that will help, in the case of hybrid cars, in greater efficiency of fossil fuel, helping to conserve the environment with a sustainable development system.

The identification of energy loss of friction braking systems in pin-on-disc tests determined that, if we use a regenerative braking system at this critical point, these two systems work better together. Regenerative brakes reduce energy loss, but they are not designed to be the only braking system on a vehicle. Their effectiveness was limited at low speeds, and they simply cannot stop a vehicle suddenly. They also cannot be used as a parking brake to prevent a parked car from rolling downhill. (Das et al., 2017). Finally, two-wheel drive vehicles do not have four-wheel drive motors; therefore regenerative braking cannot be used on the other two wheels of the vehicle.

Working together, traditional or friction brakes provide the safety factor of allowing sudden stops, while regenerative brakes reduce the temperature, pressure, and the number of times friction brakes must be used. (Ishizaka et al., 2017; Zhang et al., 2016). As vehicles fitted with regenerative brakes use friction brakes less frequently, brake dust and emissions will be reduced, but the build-up of a uniformly transferred layer of wear particles, necessary to achieve full torque in the engine, will be reduced, and total or partial braking moment. (Kumar et al., 2018)

Pin on disc tribological tests for hydraulic braking systems in a frictional contact in controlled media with the presence of a third body in the contact such as a contaminant or wet condition has been exceeded to test regenerative braking systems. This test requires modifications to conform to the new combined friction and regenerative brake standards (under SAE J2789, SAE J2707, SAE J2784, SAE J2923, SAE J2522, and SAE J2521). The tests require adjustments to include tests at lower temperatures and different braking profiles. The new dynamometers must be able to reproduce the combined effects of both braking systems at the same time with the generation of spectrum signals in real-time.

However, full-scale dynamometer testing is expensive, time-consuming, and highly trained staff involved in research to interpret the output data that will be used by peers in other disciplines to program electronic systems to investigate the optimization of the combined system to be able to propose a profitable automotive patent that allows mass production and cheaper technologies such as friction brakes. At present, countries with great technological developments have generated, together with their most specialized Technologists, machines that propose solutions to modern industry and that, in a perfect balance between Applied Research - Industry - Government, develop test benches that revolutionize technology.

Nowadays, Countries with great technological developments have generated, together with their most specialized Technologists, machines that propose solutions to modern industry and that, in a perfect balance between Applied Research - Industry - Government, develop test benches that revolutionize technology. The Model M3000 Brake Dynamometer allows testing of conventional, electro-hydraulic, electro-mechanical, regenerative hybrid-hydraulic systems. It is equipped with a DC drive motor, which allows a wide range of rotational speeds to be reached up to 2500 rpm, allowing a wide range of vehicles to be tested up to their maximum speed, in some cases 350 km/h., even plus. The M3000 allows the dynamic inertia simulation in the range of 5 kgm^2 to 250 kgm^2.

This means that we can test a wide range of vehicles, from light passenger cars, and heavy SUVs, to light commercial vehicles. This can break with a braking torque of up to 5650 N-m, which allows doing 10 m/s^2 for all the mentioned vehicles and much more for some lighter ones. See figure 02.

The station data acquisition of the M3000 allows to record in real-time on the timeline the following signals: braking torque, rotational speed, linear speed, deceleration, mechanical vibrations, dynamic unbalance, relative and absolute humidity, pad temperature, disc temperature, drum temperature, generator temperature, brake pressure, acceleration, fluid displacement, actual inertia, cooling the air temperature, cooling airflow high-speed camera image, thickness variation of the disk, peak noise level, peak noise frequency, peak noise duration, data acquisition and analysis, all signals can be recorded in real-time and on the timeline, signals can be stored with frequency up to 1000 Hz, free online technical support to analyze the results and compare them with the data obtained in other friction material.

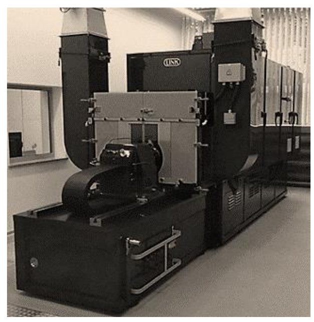

Figure 2 M3000 Brake Dynamometer for brake testing
Source: BOSMAL Automotive Research and Development Institute Ltd (2022)

Making the test procedure easier is possible on a small scale using M3000 tribometers. This saves time, and financial resources, and enables early sorting of materials, without the need for large-scale component evaluation. (Huang et al., 2017; Ishizaka et al., 2017). Another advantage of this approach is the ability to precisely control critical parameters on an internationally certified machine. (Campuzano-García et al., 2022; Soto & Montañez, 2022).

ISSN: 2410-3438

Article Journal of Quantitative and Statistical Analysis
June 2022, Vol.9 No.24 23-31

Results discussion

Hydraulic friction brakes have many recommendations in favor. They are a very effective means of providing the large amounts of braking torque needed to stop a vehicle. They are also relatively cheap and generally very reliable. However, because they depend on the act of pressing a friction material against a moving surface, the physical characteristics intelligently change over time by the rheological conditions of the compression fluid, depending on the user's driving conditions. the environment and unpredictable media, although they do not regenerate the heat energy produced by them, they are currently used as a means of braking in hybrid-electric cars due to their simplicity, economy, and responsiveness, complying with GNC systems. (Good, Nice, and Cheap), which is not that they are of poor quality, because the theories indicate that high-quality systems are expensive for having gone through a whole testing process, however, these systems have passed all those quality tests for decades and have passed them. These hydraulic braking systems are one step ahead of where the technology has been transferred and made cheaper by mass production in the automotive industry.

The contaminants layers in the contact reduce the frictional forces and increase slippage, but as the contact passes, a contaminant expulsion sweep was generated, recovering the real area of contact and adhesion with a laminar layer of wear particles that standardize: temperature transmission by conduction to the brake pad and the friction coefficient in the entire contact area.

An increase in the hydraulic pressure of the contact braking systems increases the acoustic emission, but if a third body appears in the contact, the acoustic emissions are tripled due to the slippage that it presents in the contact and the friction coefficient decreases.

It was considered that 80% of the heat generated by friction in the disc was dissipated through the phenomena of heat transfer by conduction, convection, and radiation. If this braking energy converted into heat energy is stopped so that it is not converted into heat but into rotational energy in the opposite direction to that of the braking disc, it can produce a torque in a synchronous generator system that, when the turns are cut, can supply electrical energy. On the other hand, the friction braking system will not heat up, because the regenerative system will slow down the rotation and the disc brake pad friction system now become auxiliary or emergency in case of sudden braking or at low speeds where the regenerative braking system did not reach its activation.

Regenerative braking systems currently represent a technological challenge that until now is under development and is only used in test prototypes for idealistic conditions with established parameters such as infrastructure and racing cars. These test conditions have simplified the reaction algorithm of the electronic systems that activate and deactivate the regenerative braking system. (delimitation of the study problem).

The proposal of advanced tribological machinery is a reality, but also high-cost specialized machinery with a whole set of physical infrastructure requirements, of specialized personnel to be able to operate them and exploit a whole set of technological contributions to the automotive sector. These systems may represent a set of capitalization opportunities when a good business vision is combined, a business plan for a Department of Technological Development specialized in braking systems of the private industry, the Automotive Industry, or for a Technological Development Center University that through its laboratories comply with the certifications that demonstrate its competence of services under international standards ISO 9001 and/or that its results are valid and repeatable (international accreditation ISO 17025), IEC 17025: 2017 or its Mexican equivalent, the NMX-EC-17025-IMNC-2018 standard, EMA (Mexican accreditation entity, A.C.), together with the Good Laboratory Practices (GLP) of the Organization for Economic Cooperation and Development (OECD).

ISSN: 2410-3438

But for an Engineering Educational Center this type of equipment in its laboratory represents an unattainable investment for many and in addition to lacking laboratory certifications that allow services to be sold to the business sector and are little used to carry out laboratory practices of related subjects, for what is recommended for these last Centers, the manufacture of their machinery based on the knowledge of the technologies developed in first world countries or the purchase of essential branded pin on disc equipment for pedagogical purposes so that engineering students can understand how: do they work. Once engineering students can understand how specialized equipment is tested or developed, they will need to continue to specialize so that when they come into contact with a specialized team of this magnitude they can develop patent-worthy contribution technologies among their peers. Without forgetting that the technological advance in this equipment is by leaps and bounds, the high technology centers with certified laboratories will have around 3 to 5 years to exploit them technologically, after this time it represents test equipment that for the world of research and technological development is obsolete. But it may be enabled for teaching.

Conclusions

Tribological improvements in automotive systems generate energy savings of around 18.6%. As with traditional brakes, tribology and friction reduction play an important role in regenerative brakes. Future engineering and current research aim to combine friction and regenerative brakes to minimize energy loss and maximize effectiveness. As regenerative brakes continue to evolve, friction brakes may one day become obsolete. SAE is developing tests that measure the combined performance of traditional and regenerative brakes under SAE J2789, SAE J2707, SAE J2784, SAE J2923, SAE J2522, and SAE J2521 standards.

Acknowledgments

To the Benemérita Universidad Autónoma de Puebla; Engineering Faculty for the support in the use of its infrastructure., To the Tribology and Transport Group, BUAP, for their support in the analysis and development of the work, and 189 Disaster Prevention, Sustainable Development and Tribology Academic body, BUAP.

References

Bauer H. (2019). “Automotive electrics, automotive electronics,” professional engineering, L.I. Farfan-Cabrera Tribology International 138 (2019) 473–486483 bury st. Edmunds. 2004. Retrieved August 16, 2022.

Benalcázar, M., & Gabriela, J. (2022). Caracterización y modelización de los fenómenos triboquímicos en la interfaz pastilla/rotor relacionados con el uso de sulfuros sintéticos mixtos en materiales de fricción sin cobre. Universitat de Barcelona. Retrieved August 28, 2022 from http://hdl.handle.net/2445/186065

Benedetti Matteo, et al. (2017). Investigation of lubricated rolling sliding behaviour of WC/C, WC/C-CrN, DLC based coatings and plasma nitriding of steel foro possible use in Word gea ring. Lear 2017;378–379:106–13. https://doi.org/10.1016/j. wear. 2017.02.029. Retrieved August 16, 2022

BOSMAL Automotive Research and Development Institute Ltd (2022). https://www.bosmal.eu/44-institute. Retrieved August 16, 2022.

Campuzano-García, J. Á., Braulio-Sánchez, M., Díaz-Medina, J. D., González-Durán, J. E. E., & Durán-Reséndiz, P. (2022). Diseño y desarrollo de máquina de desgaste tipo pin on ring. Revista de Ciencias Tecnológicas, 5(1), 105–120. https://doi.org/10.37636/recit.v51105120. Retrieved August 28, 2022

Champi, T., & Abel, C. (2022). Diseño de un programa de mantenimiento preventivo y su impacto económico en la Empresa Genesur E.I.R.L., Arequipa - 2021. Universidad Autónoma San Francisco. Retrieved August 28, 2022 from http://repositorio.uasf.edu.pe/handle/UASF/694

Das, Shekhar Himadry, et al. (2017). Fuel cell hybrid electric vehicles: a review on power conditioning units and topologies. Renew Sustain Energy Rev 2017; 76:268–91. https://doi.org/10.1016/j.rser.2017.03.056. Retrieved August 16, 2022.

Fernandes Marcelo Ac. (2016). Fuzzy controller applied to electric vehicles with continuously variable transmission. Neurocomputing 2016; 214:684–91. https://doi. org/10.1016/j.neucom.2016.06.051. Retrieved August 16, 2022.

Gong Ran, et al. (2015). Experimental investigation on frictional behavior and sealing performance of different composites for seal application. Wear 2015;342–343:334–9. https://doi.org/10.1016/j.wear.2015.10.001. Retrieved August 16, 2022.

Huang Chung-Neng, Chen Yui-Sung. (2017). Design of magnetic flywheel control for performance improvement of fuel cells used in vehicles. Energy 2017; 118:840–52. https://doi.org/10.1016/j.energy.2016.10.112. Retrieved August 16, 2022.

Huang Hai B, et al. (2019). Novel method for identifying and diagnosing electric vehicle shock absorber squeak noise based on a DNN. Mech Syst Signal Process 2019; 124:439–58. https://doi.org/10.1016/j.ymssp.2019.01.053. Retrieved August 16, 2022.

Ishizaka Kei, et al. (2017). The low adhesion problem due to leaf contamination in the wheel/rail contact: bonding and low adhesion mechanisms. Wear 2017;378–379:183–97. https://doi.org/10.1016/j.wear.2017.02.044. Retrieved August 16, 2022.

Kumar K Mohan, et al. (2018). Tribology of silicon surfaces: a review. Mater Today: Proceedings 2018;5(11):24809–19. https://doi.org/10.1016/j.matpr.2018.10. 279. Retrieved August 16, 2022.

Li Jitai, et al. (2018). Impact of polydimethylsiloxanes on physicochemical and tribological properties of naphthenic mineral oil (KN 4010)-based titanium complex grease. Chin J Chem Eng 2018. https://doi.org/10.1016/j.cjche.2018.09.002. Retrieved August 16, 2022.

Lugt Piet M. (2016). Modern advancements in lubricating grease technology. Tribol Int 2016; 97:467–77. https://doi.org/10.1016/j.triboint.2016.01.045. Retrieved August 16, 2022.

Ma Z & Zhan C. (2015). System stability and control strategy of electric power steering. Presented at the International Conference on logistics, engineering, management and computer science. Shenyang, China: LEMCS 2015); 2015. Retrieved August 16, 2022 from https://doi.org/10.2991/lemcs-15.2015.58

Mukoyama Shinichi, et al. (2017). Development of superconducting magnetic bearing for 300 KW flywheel energy storage system. IEEE Trans Appl Supercond 2017;27(4):1–4. https://doi.org/10.1109/tasc.2017.2652327. Retrieved August 16, 2022.

Nuñez, A., & Andree, H. (2022). Gestión del plan de lubricación para disminuir el impacto con la disponibilidad de camiones de acarreo de 400 toneladas en minera Antamina. Universidad Nacional de San Agustín de Arequipa. Retrieved August 28, 2022 from http://hdl.handle.net/20.500.12773/14441

Shababi Kianoosh, et al. (2017). An experimental study on rheological behavior of SAE50 engine oil. J Therm Anal Calorim 2017;131(3):2311–20. https://doi.org/10.1007/ s10973-017-6693-6. Retrieved August 16, 2022.

Soto López, D. J., & Montañez Bohórquez, J. D. (2022). Elaboración de una propuesta para implementar un sistema de mantenimiento inteligente. Caso de estudio: una flota del SITP del fabricante Daimler Colombia S.A. https://repositorio.ecci.edu.co/handle/001/2500. Retrieved August 28, 2022

Stoica N A and Tudor A. (2015). Some aspects concerning the behaviour of friction materials at low and very low sliding speeds Tribology in Industry 37 374-79. Retrieved August 16, 2022.

Syahir AZ. (2017). A review on bio-based lubricants and their applications. J Clean Prod 2017; 168:997–1016. Retrieved August 16, 2022 from https://www.sciencedirect.com/science/article/abs/pii/S0959652617320966

Tormos Bernardo, et al. (2017). Fuel consumption and friction benefits of low viscosity engine oils for heavy duty applications. Tribol Int 2017; 110:23–34. https://doi.org/10.1016/j.triboint.2017.02.007. Retrieved August 16, 2022.

Wicki Samuel, Erik G. (2017). Hansen. “Clean energy storage technology in the making: an innovation systems perspective on flywheel energy storage. J Clean Prod 2017; 162:1118–34.
https://doi.org/10.1016/j.jclepro.2017.05.132.
Retrieved August 16, 2022.

Zhang Jie, et al. (2016). The application of PTFE coating on spherical joints. Proceedings of the 2015 2nd internatisonal conference on machinery, materials engineering, chemical engineering and biotechnology 2016. https://doi.org/10.2991/mmecebL.I. Farfan-Cabrera Tribology International 138 (2019) 473–48648515.2016.139. Retrieved August 16, 2022.

Zhang Zutao, et al. (2016). A high-efficiency energy regenerative shock absorber using supercapacitors for renewable energy applications in range extended electric vehicle. Appl Energy 2016; 178:177–88. https://doi.org/10.1016/j.apenergy.2016.06.054. Retrieved August 16, 2022.

Zhao Bin, et al. (2018). Stability control of electric vehicles with in-wheel motors by considering tire slip energy. Mech Syst Signal Process 2019; 118:340–59. https://doi.org/10.1016/j.ymssp.2018.08.037.
Retrieved August 16, 2022.

Article **Journal of Quantitative and Statistical Analysis**
Month, Year Vol.1 No.1 1-15-[Using ECORFAN]

[Title in Times New Roman and Bold No. 14 in English and Spanish]

Surname (IN UPPERCASE), Name 1st Author†*, Surname (IN UPPERCASE), Name 1st Coauthor, Surname (IN UPPERCASE), Name 2nd Coauthor and Surname (IN UPPERCASE), Name 3rd Coauthor

Institutional Affiliation of Author including Dependency (No.10 Times New Roman and Italic)

International Identification of Science - Technology and Innovation

ID 1st Author: (ORC ID - Researcher ID Thomson, arXiv Author ID - PubMed Author ID - Open ID) and CVU 1st author: (Scholar-PNPC or SNI-CONACYT) (No.10 Times New Roman)

ID 1st Coauthor: (ORC ID - Researcher ID Thomson, arXiv Author ID - PubMed Author ID - Open ID) and CVU 1st coauthor: (Scholar or SNI) (No.10 Times New Roman)

ID 2nd Coauthor: (ORC ID - Researcher ID Thomson, arXiv Author ID - PubMed Author ID - Open ID) and CVU 2nd coauthor: (Scholar or SNI) (No.10 Times New Roman)

ID 3rd Coauthor: (ORC ID - Researcher ID Thomson, arXiv Author ID - PubMed Author ID - Open ID) and CVU 3rd coauthor: (Scholar or SNI) (No.10 Times New Roman)

(Report Submission Date: Month, Day, and Year); Accepted (Insert date of Acceptance: Use Only ECORFAN)

Abstract (In English, 150-200 words)

Objectives
Methodology
Contribution

Keywords (In English)

Indicate 3 keywords in Times New Roman and Bold No. 10

Abstract (In Spanish, 150-200 words)

Objectives
Methodology
Contribution

Keywords (In Spanish)

Indicate 3 keywords in Times New Roman and Bold No. 10

Citation: Surname (IN UPPERCASE), Name 1st Author, Surname (IN UPPERCASE), Name 1st Coauthor, Surname (IN UPPERCASE), Name 2nd Coauthor and Surname (IN UPPERCASE), Name 3rd Coauthor. Paper Title. Journal of Quantitative and Statistical Analysis. Year 1-1: 1-11 [Times New Roman No.10]

* Correspondence to Author (example@example.org)
† Researcher contributing as first author.

Introduction

Text in Times New Roman No.12, single space.

General explanation of the subject and explain why it is important.

What is your added value with respect to other techniques?

Clearly focus each of its features

Clearly explain the problem to be solved and the central hypothesis.

Explanation of sections Article.

Development of headings and subheadings of the article with subsequent numbers

[Title No.12 in Times New Roman, single spaced and bold]

Products in development No.12 Times New Roman, single spaced.

Including graphs, figures and tables-Editable

In the article content any graphic, table and figure should be editable formats that can change size, type and number of letter, for the purposes of edition, these must be high quality, not pixelated and should be noticeable even reducing image scale.

[Indicating the title at the bottom with No.10 and Times New Roman Bold]

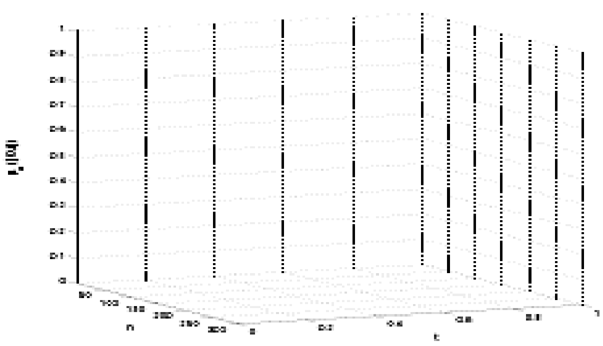

Graphic 1 Title and *Source (in italics)*

Should not be images-everything must be editable.

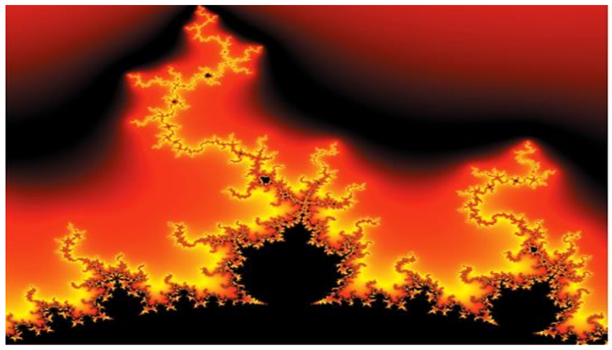

Figure 1 Title and *Source (in italics)*

Should not be images-everything must be editable.

Table 1 Title and *Source (in italics)*

Should not be images-everything must be editable.

Each article shall present separately in **3 folders**: a) Figures, b) Charts and c) Tables in .JPG format, indicating the number and sequential Bold Title.

For the use of equations, noted as follows:

$$Y_{ij} = \alpha + \sum_{h=1}^{r} \beta_h X_{hij} + u_j + e_{ij} \qquad (1)$$

Must be editable and number aligned on the right side.

Methodology

Develop give the meaning of the variables in linear writing and important is the comparison of the used criteria.

Results

The results shall be by section of the article.

Annexes

Tables and adequate sources

Thanks

Indicate if they were financed by any institution, University or company.

Conclusions

Explain clearly the results and possibilities of improvement.

References

Use APA system. Should not be numbered, nor with bullets, however if necessary numbering will be because reference or mention is made somewhere in the Article.

Use Roman Alphabet, all references you have used must be in the Roman Alphabet, even if you have quoted an Article, book in any of the official languages of the United Nations (English, French, German, Chinese, Russian, Portuguese, Italian, Spanish, Arabic), you must write the reference in Roman script and not in any of the official languages.

Technical Specifications

Each article must submit your dates into a Word document (.docx):

Journal Name
Article title
Abstract
Keywords
Article sections, for example:

1. Introduction
2. Description of the method
3. Analysis from the regression demand curve
4. Results
5. Thanks
6. Conclusions
7. References

Author Name (s)
Email Correspondence to Author
References

Intellectual Property Requirements for editing:

- Authentic Signature in Color of Originality Format Author and Coauthors.

- Authentic Signature in Color of the Acceptance Format of Author and Coauthors.

- Authentic Signature in blue colour of the Conflict of Interest Format of Author and Co-authors.

Reservation to Editorial Policy

Journal of Quantitative and Statistical Analysis reserves the right to make editorial changes required to adapt the Articles to the Editorial Policy of the Journal. Once the Article is accepted in its final version, the Journal will send the author the proofs for review. ECORFAN® will only accept the correction of errata and errors or omissions arising from the editing process of the Journal, reserving in full the copyrights and content dissemination. No deletions, substitutions or additions that alter the formation of the Article will be accepted.

Code of Ethics - Good Practices and Declaration of Solution to Editorial Conflicts

Declaration of Originality and unpublished character of the Article, of Authors, on the obtaining of data and interpretation of results, Acknowledgments, Conflict of interests, Assignment of rights and Distribution

The ECORFAN-Mexico, S.C Management claims to Authors of Articles that its content must be original, unpublished and of Scientific, Technological and Innovation content to be submitted for evaluation.

The Authors signing the Article must be the same that have contributed to its conception, realization and development, as well as obtaining the data, interpreting the results, drafting and reviewing it. The Corresponding Author of the proposed Article will request the form that follows.

Article title:

– The sending of an Article to Journal of Quantitative and Statistical Analysis emanates the commitment of the author not to submit it simultaneously to the consideration of other series publications for it must complement the Format of Originality for its Article, unless it is rejected by the Arbitration Committee, it may be withdrawn.

– None of the data presented in this article has been plagiarized or invented. The original data are clearly distinguished from those already published. And it is known of the test in PLAGSCAN if a level of plagiarism is detected Positive will not proceed to arbitrate.

– References are cited on which the information contained in the Article is based, as well as theories and data from other previously published Articles.

– The authors sign the Format of Authorization for their Article to be disseminated by means that ECORFAN-Mexico, S.C. In its Holding Bolivia considers pertinent for disclosure and diffusion of its Article its Rights of Work.

– Consent has been obtained from those who have contributed unpublished data obtained through verbal or written communication, and such communication and Authorship are adequately identified.

– The Author and Co-Authors who sign this work have participated in its planning, design and execution, as well as in the interpretation of the results. They also critically reviewed the paper, approved its final version and agreed with its publication.

– No signature responsible for the work has been omitted and the criteria of Scientific Authorization are satisfied.

– The results of this Article have been interpreted objectively. Any results contrary to the point of view of those who sign are exposed and discussed in the Article.

Copyright and Access

The publication of this Article supposes the transfer of the copyright to ECORFAN-Mexico, SC in its Holding Bolivia for it Journal of Quantitative and Statistical Analysis, which reserves the right to distribute on the Web the published version of the Article and the making available of the Article in This format supposes for its Authors the fulfilment of what is established in the Law of Science and Technology of the United Mexican States, regarding the obligation to allow access to the results of Scientific Research.

Article Title:

Name and Surnames of the Contact Author and the Coauthors	Signature
1.	
2.	
3.	
4.	

Principles of Ethics and Declaration of Solution to Editorial Conflicts

Editor Responsibilities

The Publisher undertakes to guarantee the confidentiality of the evaluation process, it may not disclose to the Arbitrators the identity of the Authors, nor may it reveal the identity of the Arbitrators at any time.

The Editor assumes the responsibility to properly inform the Author of the stage of the editorial process in which the text is sent, as well as the resolutions of Double-Blind Review.

The Editor should evaluate manuscripts and their intellectual content without distinction of race, gender, sexual orientation, religious beliefs, ethnicity, nationality, or the political philosophy of the Authors.

The Editor and his editing team of ECORFAN® Holdings will not disclose any information about Articles submitted to anyone other than the corresponding Author.

The Editor should make fair and impartial decisions and ensure a fair Double-Blind Review.

Responsibilities of the Editorial Board

The description of the peer review processes is made known by the Editorial Board in order that the Authors know what the evaluation criteria are and will always be willing to justify any controversy in the evaluation process. In case of Plagiarism Detection to the Article the Committee notifies the Authors for Violation to the Right of Scientific, Technological and Innovation Authorization.

Responsibilities of the Arbitration Committee

The Arbitrators undertake to notify about any unethical conduct by the Authors and to indicate all the information that may be reason to reject the publication of the Articles. In addition, they must undertake to keep confidential information related to the Articles they evaluate.

Any manuscript received for your arbitration must be treated as confidential, should not be displayed or discussed with other experts, except with the permission of the Editor.

The Arbitrators must be conducted objectively, any personal criticism of the Author is inappropriate.

The Arbitrators must express their points of view with clarity and with valid arguments that contribute to the Scientific, Technological and Innovation of the Author.

The Arbitrators should not evaluate manuscripts in which they have conflicts of interest and have been notified to the Editor before submitting the Article for Double-Blind Review.

Responsibilities of the Authors

Authors must guarantee that their articles are the product of their original work and that the data has been obtained ethically.

Authors must ensure that they have not been previously published or that they are not considered in another serial publication.

Authors must strictly follow the rules for the publication of Defined Articles by the Editorial Board.

The authors have requested that the text in all its forms be an unethical editorial behavior and is unacceptable, consequently, any manuscript that incurs in plagiarism is eliminated and not considered for publication.

Authors should cite publications that have been influential in the nature of the Article submitted to arbitration.

Information services

Indexation - Bases and Repositories

LATINDEX (Scientific Journals of Latin America, Spain and Portugal)
RESEARCH GATE (Germany)
GOOGLE SCHOLAR (Citation indices-Google)
REDIB (Ibero-American Network of Innovation and Scientific Knowledge- CSIC)
MENDELEY (Bibliographic References Manager)

Publishing Services:

Citation and Index Identification H.
Management of Originality Format and Authorization.
Testing Article with PLAGSCAN.
Article Evaluation.
Certificate of Double-Blind Review.
Article Edition.
Web layout.
Indexing and Repository
ArticleTranslation.
Article Publication.
Certificate of Article.
Service Billing.

Editorial Policy and Management

21 Santa Lucía, CP-5220. Libertadores -Sucre–Bolivia. Phones: +52 1 55 6159 2296, +52 1 55 1260 0355, +52 1 55 6034 9181; Email: contact@ecorfan.org www.ecorfan.org

ECORFAN®

Chief Editor
MIRANDA - TORRADO, Fernando. PhD

Executive Director
RAMOS-ESCAMILLA, María. PhD

Editorial Director
PERALTA-CASTRO, Enrique. MsC

Web Designer
ESCAMILLA-BOUCHAN, Imelda. PhD

Web Diagrammer
LUNA-SOTO, Vladimir. PhD

Editorial Assistant
TREJO-RAMOS, Iván. BsC

Philologist
RAMOS-ARANCIBIA, Alejandra. BsC

Advertising & Sponsorship

(ECORFAN® Bolivia), sponsorships@ecorfan.org

Site Licences

03-2010-032610094200-01-For printed material ,03-2010-031613323600-01-For Electronic material,03-2010-032610105200-01-For Photographic material,03-2010-032610115700-14-For the facts Compilation,04-2010-031613323600-01-For its Web page,19502-For the Iberoamerican and Caribbean Indexation,20-281 HB9-For its indexation in Latin-American in Social Sciences and Humanities,671-For its indexing in Electronic Scientific Journals Spanish and Latin-America,7045008-For its divulgation and edition in the Ministry of Education and Culture-Spain,25409-For its repository in the Biblioteca Universitaria-Madrid,16258-For its indexing in the Dialnet,20589-For its indexing in the edited Journals in the countries of Iberian-America and the Caribbean, 15048-For the international registration of Congress and Colloquiums. financingprograms@ecorfan.org

Management Offices

21 Santa Lucía, CP-5220. Libertadores -Sucre–Bolivia.

Journal of Quantitative and Statistical Analysis

"Photoluminescence comparison of CNTs-SRO and GO-SRO films deposited on silicon substrates"
MENDOZA-CONDE, Gabriel Omar, LUNA-LÓPEZ, José Alberto, HERNÁNDEZ-SIMÓN, Zaira Jocelyn and HERNÁNDEZ-DE LA LUZ, José Álvaro David
Benemérita Universidad Autónoma de Puebla

"Analysis of the behavior for polyethylene terephthalate (PET) in compression efforts for use in the masonry"
VEGA-GUTIÉRREZ, Rebeca Eloísa, MARTÍNEZ-CARRILO, Irma, JUÁREZ-TOLEDO, Carlos and JIMÉNEZ-BETANCOURT, Ramón Octavio
Universidad Autónoma del Estado de México
Universidad Autónoma de Colima

"Thermodynamic analysis of a Stirling cycle with nuclear heat source for aerospace applications"
DÍAZ-ESPINOZA, Gerardo, GALLARDO-VILLARREAL, José Manuel and VALLE-HERNÁNDEZ, Julio
Universidad Politécnica Metropolitana de Hidalgo
Universidad Autónoma del Estado de Hidalgo

"Brake systems tribological analysis and their evolution in sustainable characterization"
LAGOS-LÓPEZ, Lorena, CRUZ-GOMEZ, Marco Antonio, MEJÍA-PÉREZ, José Alfredo and ESPINOSA-CARRASCO, María del Rosario
Benemérita Universidad Autónoma de Puebla

2410 3438
ISSN 2410 - 3438
www.ecorfan.org